PROJECT FINAL REPORT

Publishable Summary

Grant Agreement number: 221952

Project acronym: ATLAS

Project title: Development of Laser-Based Technologies and Prototype Instruments for Genome-Wide Chromatin ImmunoPrecipitation Analyses

Funding Scheme: Collaborative Action

Period covered: from 1April 2009 to 30 September 2012

Project co-ordinator name and title: Prof. Lucia Altucci

Organisation: Second University of Naples, Italy

Tel: +39-0815667569

Fax: +39-0812144840

E-mail: lucia.altucci@unina2.it

Project website address: www.atlas-eu.com

Final publishable summary report

Executive summary

The knowledge of mechanisms leading the interactions among bio-molecules in living cells represents one of the main goal in molecular biology in order to define the dynamics of (direct and indirect) bindings. Currently, the establishment of a stable inter-play between nucleic acid and proteins (in particular DNA-proteins crosslink) is mainly obtained through the conventional chemical methods involving the use of a bifuctional reagent, for instance, the formaldehyde. Protein-DNA interactions play an important role in DNA replication, recombination, repair and, consequently, in transcriptional and translational gene regulation. The modulation of chromatin structure is a complex and dynamic process regulated at multiple levels though distinct mechanisms such as histone post-translational modifications, non-coding RNA and DNA methylation. Aberrations of gene regulation might lie in pathological chromatin status. The establishment of a standing covalent bond between proteins and nucleic acids (crosslinking) open access to the study of interactions between bio-molecules: this is a crucial task for understanding functions and deregulation of gene expression. Enzymatic methods to examine protein-DNA interactions, have been developed in *vivo* and in *vitro* though genomic foot-printing. Recently, Chromatin ImmunoPrecipitation (ChIP) assay allows to identify both the binding patterns between transcription factors (TFs) and chromatin and to evaluate the occurence of histone modifications. Despite the needs, the current ChIP technology does not allow to discriminate either direct or indirect binding or to study transient chromatin occupancy. Indeed specific bond of transcription factors (TFs) causes in a large part the connectivity of gene regulatory networks as well as the quantitative level of gene expression. In order to satisfy these requirements, a new and more efficient crosslink reaction, based on the employment of an UV laser source, was developed. The use of UV laser crosslinking thus represents an innovative way to create a stable covalent bond though the excitation of the electronic state of proteins and DNA. UV irradiation creates covalent bindings between the reactive groups of DNA (thymine and cysteine) and amino acids (serine, methionine, lysine, arginine, histidine, tryptophan, phenylalanine or tyrosine). Therefore, the occurrence of a crosslink is accompanied by a combination of factors, including the inherent photo-reactivity of the excited nucleotides, the geometrical arrangement and the molecular dynamics involved in the mechanism of crosslink. UV light is a zero length crosslinker and produces less perturbation of the complex than chemical crosslinker such as formaldehyde.

UV Laser-based chromatin immunoprecipitation (LChIP) induces photo-mediated crosslink in a very short time allowing the study of transient interactions by varying different parameters such as energy, repetition rate and pulse intensity in time unit. UV irradiation of cells at the wavelength of about 260 nm produces covalent bonds in nucleic acids and proteins and, in particular, may preferentially allow bonds between TFs and histones associated within chromatin.

So, LChIP is able to characterize the dynamics of the transcription factors binding on chromatin in living cells because the required time for Laser-mediated crosslink is several orders of magnitude lower than the conventional methods. This technique makes available the study of temporal and spatial bindings of proteins on DNA and so, it becames a usefull tool for understanding regulation of gene expression and maintenance. Although living human cells non-linearly respond to irradiation with intense fs-UV-laser pulses, among the phenomena triggered by such pulses, a highly efficient DNA-proteins relationship occurs.

Definitively, the development of LChIP technique and its applications have the powerful potential in detecting the behaviour of transient DNA-proteins bindings in *vivo*. The study of these transient interactions in a short time scale, a parameter undetectable with conventional methodologies, is now possible corroborating the extraordinary biomedical potential of LChIP for discriminating chromatin epigenome and TF bindings dynamically.

Summary description of project context and objectives

The availability of the DNA sequence of many eukaryotic genomes and the generation of high density tiling arrays covering such entire genomes has made it possible to decipher the regulatory principles that are based on the interplay of *trans*-regulatory TFs and their cognate *cis*-regulatory DNA recognition sequences at genome-wide level. At chromatin level a mutual interplay between TFs and epigenetic modifiers (DNA and histone modifying machinaries) sets up determinants of gene (in)activity. The ensemble of histone modifications at a given gene locus has been proposed to establish an "epigenetic code" of great complexity. Irrespectively of whether such a code does exist or whether chromatin modifications rather constitute a step in signal transduction, it has become increasingly clear that chromatin modifications constitute docking sites for regulatory factors. Thus, description of the information encoded by genomes requires a deconvolution of the genetic and epigenetic programs and the interplay between these two regulatory levels. In addition to their enormous potential and power for the study of gene regulation mechanisms such analyses also provide important tools for diagnosis, prognosis, and therapy of diseases. Decoding chromatin-embedded information at the whole genome level by combining ChIP with global analysis such as DNA tiling arrays (ChIP-chip or ChIP-on-chip) or parallel single molecule sequencing, ChIP-seq, have become powerful approaches currently applied to mammalian genomes to analyze gene regulation programs. Global ChIP analyses allow converting genomic information into a dynamic regulatory network that operates in a time, cell, development and environment-dependent manner to coordinate cell homeostasis, proliferation, survival and death, as well as cell-cell comunication. *ChIP* is a powerful approach to determine *in vivo* the chronology of TFs recruitment during activation or repression in the context of chromatin and changes in epigenetic signatures and chromatin remodeling. In many applications, protein and DNA are cross-linked using formaldehyde, chromatin is fragmented, and the protein of interest is immunoprecipitated with specific antibodies (*XChIP*). Alternatively, native ChIP (*NChIP*) i.e. without chemical crosslinkers, can be used in epigenetic profiling studies. The relative amount of a particular DNA fragment cross-linked to the protein (and therefore present in the precipitate) is determined by qPCR, and is a measure of the occupancy of the factor at that particular position in the genome.

Despite providing significant insight in transcription regulation and chromatin-mediated effects, NChIP and XChIP technologies have a number of intrinsic technical limitations. These comprise:

Selectivity: Formaldehyde introduces covalent bonds between protein-DNA and protein-protein. TFs are generally embedded within complexes/machineries that display multiple interaction surfaces (with DNA or between subunits). This has two consequences: (i) factors that bind DNA directly or indirectly via protein-protein interactions with chromatin components will be crosslinked with widely different efficiencies depending on the stability of the interaction and (ii) a single protein/complex can be crosslinked to more than one site in the genome e.g. in the case of enhancer-promoter looping. NChIP can only be employed efficiently for very stable interactions, predominantly histone (nucleosome)-DNA interactions.

Accuracy and efficiency: The overall performance of XChIP depends critically on the efficiency of the first step, the crosslink of factors to DNA by formaldehyde exposure of living cells. However, chemical crosslinking is diffusion-controlled and varies considerably with cell type, manipulation, storage and purity of the chemical. Due to the progressively increasing non-specific crosslink by chemical crosslinkers, formaldehyde crosslinking has to be stopped a long time before a maximal crosslinking of DNA to protein has been reached. This implies low efficiency of the subsequent immunoprecipitation.

Dynamics and half-lifes of DNA interactions: TFs bind with highly different kinetics/half-lives to DNA/chromatin. Current technologies do not allow studying very short-live interactions. It is, for example, not possible to resolve the "DNA/chromatin scanning" model of a TF as opposed to a "direct recruitment" model. Data obtained in XChIP (co)factor binding studies e.g. on the time-resolved Estrogen Receptor (ER) activation poorly correlates with photo-bleaching experiments resulting in a controversy about the actual molecular mechanisms of TF action.

Sensitivity: Conventional XChIP requires large amounts of cells (about 10^6 to 10^8 cells) as starting material. A significantly higher sensitivity (down to 1,000

cells) has been reported for carrier ChIP (CChIP) that involves NChIP procedure for the analysis of histone modification. However, this procedure is not applicable to TF interactions with DNA/chromatin.

Single cell, tissue crosslinking and sorting: Current ChIP technologies do not permit crosslink of selected individual cells or frozen tissue slides and subsequent analyses of defined population.

Epitope masking and modification: Formaldehyde crosslinking alters lysine residues, which can be part of antibody epitopes in targeted DNA binding proteins, particularly in modified histones. This has several serious drawbacks: (i) it reduces substantially the IP efficacy in epigenetic studies and yields <<1% are commonly observed3, (ii) due to the covalent stabilization of entire complexes, antibody epitopes may reside inside a complex, which would become accessible due to dissociation if only DNA crosslinks would occur, (iii) epitope-tagging is limited to peptides that are not modified by formaldehyde.

To overcome most of the above mentioned limitations, ATLAS consortium established novel ChIP technologies (LChIP) consisting in the development and subsequent creation of an experimental platform that, through the employing of a laser source, is able to induce cross-link reactions between DNA and proteins within living cells to study the evolution in time and space of both the transcriptional machinery and epigenetic code. Laser technology, therefore, represents a valid alternative to traditional methods, as it is able to induce bonds between DNA and proteins in very short intervals of time and with high efficiency. The driving idea of Atlas is the observation, confirmed by experimental data and evidences in the literature, that an ultrashort UV laser can excite the electronic states of nitrogenous bases composing the DNA and amino acid side residues of proteins that bind DNA itself. Once absorbed energy, the system DNA-protein relaxes to the ground state via the formation of a covalent bond. The creation of this link, obtained by a method "foto-physic", opens up a range of possibilities for study of interaction in "real time" and rapid decoding of "cross talk" between transcription factors, enhancers, epigenetic modulators and DNA. The reducing time scale of crosslink induction increases the number of proteins-DNA interaction that can be analyzed by “omic” science, and in general helps to clarify the temporal sequence of the events constituting the biological phenomenon (for example the epigenetic code variation). Comparing the conventional method with LChIP some drawbacks might be overcome. So, the novel LChIP technology identifies direct protein-DNA contacts preferentially if not exclusively under certain conditions (increasing of selectivity).

LChIP involves ultra-fast physical crosslinking by femtosecond UV lasers specifically designed for highly efficient DNA-protein crosslinking. Once calibrated it operates fully reproducible and highly accurate, and is cell and experimenter independent. Due to its ultra-fast crosslinking, LChIP allows fundamental studies on the mechanisms of DNA/chromatin recognition by DNA-binding regulatory factors.

Given to its high efficiency documented in proof-of-principle experiments (see sections below), LChIP linked to microscopic and cell-sorting platforms using microfluidic systems permits to photo crosslink subsets of cells ‘on-the-fly’, crosslink cells in particular phases of the cell cycle, or leukemia blasts for genome-wide analyses. In addition, LChIP does not affect protein epitopes and hence has a dramatically higher IP efficacy allowing the use of epitope-tagging approaches with highly efficient antibodies independent of the presence of lysines. To reach these aims industrial partners, mathematicians, physicists, molecular biologists, chemists and MDs worked together up to construct a prototype of a complex device, including Laser apparatus and microfluidic station, to perform induction of crosslink in living cells in an easy and not time consuming manner. The prototype is additionally governed by software, made for the Atlas purpose, with a friendly interface and it easy to understand.

In order to realize the prototype, the efforts of Atlas project were centred on two main different research lines:

- A technological one in which the construction of dedicated femtosecond double-pulse, two colors tunable laser apparatus was made, as such as the development of microfluidic and cell sorting machinery (see first part of S&T results/foreground description)

- An experimental one aimed to discover the chemical principles and mechanism of photo-crosslink and the development and validation of LChIP in cell-based assays (see second part of S&T results/foreground description).

The step-by-step progression of the Atlas project was allowed trough a series of objectives achievement. In the list below the most important ones are summarized:

- Development and validation of a custom femtosecond laser prototype for optimized UV-laser photo-induced crosslinking with high efficiency. In the first 12 months of project, a new dedicated ultrashort laser system has been developed that is be able to deliver high-energy, UV, fs-pulses (in the energy range of several microjoule per pulse) at a repetition rate variable within six orders of magnitude, between 1Hz and 1MHz. The wavelength of such pulses is variable in the range 250-280 nm, to match the first UV absorption band range of DNA bases. The combined features of high energy/pulse and high repetition rate were not commercially available at the moment of Atlas project start and until now, for any known ultrashort laser source. This is so the first prototype released in the context of Atlas project. Its realization involved the collaboration of industrial partners specialized in UV-laser source construction and commercialization as such as some university partners devoted to the management, control and improvement of Laser apparatus.
- Development and implementation of laser system upgrades with dedicated Optical Parametric Amplifier (OPA) that allows performing two-colour, double pulse irradiation of the sample, thereby significantly minimizing cell damage after the irradiation of biomolecules or living systems with UV laser source (however ensuring and optimizing DNA-protein crosslink). The developed OPA has unique features in terms of high energy/pulse together with the high pulse repetition rate and has a wide tunability, covering the 200 nm – 2600 nm spectral window. The OPA technology, although commercially existent, has been applied for the first time to Laser apparatus described above, expanding much the possible wavelengths window.
- Determination of the chemical nature of laser-induced DNA-protein cross-linking, using the synergy between theoretical calculations and study of increasingly complex chemical models, was carried out. Factors effecting the excitation of the DNA and the protein, the formation of intermediate reactive species, and the creation of the new DNA-protein bonds have been addressed in a sequential manner, from the isolated building blocks of each macromolecule to reacting adjacent monomers and the long-range effects that can be found in larger systems with tertiary structure, in particular when proximity (and affinity) is enforced. This multi-level detailed description of the photochemical behaviour of DNA in a protein environment has provide the knowledge for rational design and optimization of the crosslinking experimental conditions in cell based assays
- Evaluation of macroscopic parameters characterizing the DNA-laser interaction has been carried out in cell based assays in order to indicate the ones (such as time, geometry, cell behaviour) that mainly affect the induction of crosslink between DNA-proteins in living cells. The final benefit has consisted in indicating the values or the restricted range of values for an optimal interaction between the laser and the molecular system.
- First results of LChIP were been obtained on single gene analysis and than the skills arising from these experiments were applied to perform genome-wide studies of LChIP (LChIP-seq).
- The feasibility of LChIP was estimated by looking at particular genomic regions and well-defined transcriptional factors (or enhancers of transcription) to better decipher the evolution in time and space of transcriptional pathways and networks and the difference between direct and indirect binding of proteins to DNA.
- Integration of LChIP with microfluidic-based cell sorting platforms was obtained. Dedicated laser system has been integrated into the fluorescence-activated microfluidic cell sorter. This setup allows analysis of selective subsets using much lower number of cells than required for conventional approaches. Moreover, this approach allows the dynamic crosslinking of cells in a flux and number dependent manner.

- Application of LChIP with i) microscopic manipulations of frozen tissue slices; ii) microfluidic station for experiments in cellular subpopulations; iii) global study of epi-modifications and TFs binding in time resolved manner upon selected treatments (f.e. Epi-drugs) was performed.
- Optimization of amplification methods of very small amounts of DNA obtained by LChIP (#6), allowing the use of low numbers of cells as starting material, has been done. In parallel, another industrial partner carried out the development and characterization of antibodies to obtain LChILL and LChIP grade antibodies; in particular emphasis was on the production of antibodies against epitope peptides that will be masked by formaldehyde in order to improve the effiency of IP stage. At the same manner, kit(s) for LChIP (and for DNA amplification for LChIP) was developed. The LChIP contains controls such as LChIP grade antibodies and physically crosslinked cells as well as optimized buffers, PCR primers and adapted protocol.

As described previously, in the context of Atlas project, the borders among different scientific fields have been overcome, by joining Physics and Bio-medical approaches to answer to a typical biological question (such as “what binds what in a cellular system”) and to clarify the principles underpinning the interaction between biomolecules and UV radiation. The multidisciplinary aspect characterized strongly this project and maybe it was the keystone to develop the new LChIP technique.
ATLAS integrated dispersed capabilities of partners from 8 European countries and assembled the critical mass required to enable new global approaches, by networking the necessary expertise to secure European excellence and competitiveness, and to explore new directions in the research field. Consortium delivers new knowledge on basic biological processes relevant to health and disease.
With the new LChIp is now possible to better identify:

- ***Selective factor-DNA crosslink repertories.*** Using ATLAS technology non-specific protein-protein crosslink is negligible (under appropriate conditions) allowing, for the first time, the study of ‘bona fide’ pure bindings to chromatin with unmet accuracy. Consequently, highly precise transcription factor (or epigenetic modification) maps can be generated, potentially reflecting dynamics and kinetics of bindings. Comparison with conventional chemical crosslink facilitates to distinguish between direct and indirect (through protein-protein contacts) DNA binding. Such information is of extraordinary mechanistic value.
- ***Novel strategy of experimental design-important mechanistic question can be addressed***. The ATLAS technology could potentially change the actual view of promoter function and gene regulation, leading to novel concepts of gene expression. Indeed, the comparison with data from formaldehyde crosslinking will most likely lead to novel classification/distinction of binding sites in enhancers versus promoters and/or to a completely revised view of enhancer and promoter function. Moreover, the efficiency and specificity of this approach allows to define cellular context specific regulation in a dynamic time frame, which is currently unthinkable due to technical limitations. The applications of this technology most likely open a new strategy of experimental design with very wide applicabilities.

A description of the main S&T results/foregrounds

The overall objective of the ATLAS consortium was to develop novel types of femtosecond (fs) tunable UV lasers to induce highly efficient DNA-protein crosslinking for chromatin immunoprecipitation analyses (LChIP). LChIP overcomes the current limitations of chemical crosslink. Specific, technological objectives were to fuse a microfluidic station with the ultrashort laser source in a unique, new machine to perform dynamic crosslinking in a time and cell type and/or differentiation-specific dependent manner. The LChIP technology could also be applied on frozen tissue slices for global applications. Specific biological objectives were to adapt and optimize LChIP technology to global genome analysis or massive, parallel single molecule sequencing using Solexa - LChIP-seq.

We further applyed LChIP technologies to selected cell populations (down to the single cell level); we achieved this goal i) by connecting the Laser with a microfluidic system, which may sort out specific cell populations, and ii) by selectively focusing on cell populations in solid tissues or specimens. Finally, we developed software to automate the Laser & microfluidic station system thereby constructing a versatile and user-friendly new-dedicated machine of high commercial interest.

The development of this technology/machinery has been assessed trough technical efforts and scientific ideas that will be discussed separately in this document.

TECHNICAL RESULTS

The main goal of this activity was to develop customized laser system based on femtosecond Yb:KGW laser, optical parametric amplifier (OPA) and harmonic generators delivering two synchronized pulses at two different wavelengths from two independent channels. The UV pulse is produced by fourth harmonic (optionally third harmonic) generator installed in the first system channel. A second channel contains a continuously tuneable collinear OPA, equipped with additional tuneable frequency converters, covering the 210-515 nm range. In the first period of ATLAS project the R&D activity was concentrated on: a) general design of collinear pumped OPA with harmonic generators, b) study of broadband seed formation in a continuum generation stage, c) OPA build up and investigation of its performance, d) investigation of OPA signal conversion to UV. Here just some of these are summarized.

OPA design: OPA was designed as an two stage parametric amplifier seeded by white light continuum (WLC) and pumped by SH of ~180 fs pulses generated by Yb:KGW laser. SH generator, continuum generator, OPA stages and harmonic generators are integrated in single unit. A small portion of the incoming pulse is split off and used to generate WLC in a bulk medium. The rest of the pulse is frequency doubled and used as the pump for two OPA stages. The first OPA stage serves for pre-amplification of the spectral portion of broadband signal coming from continuum generator. The selection of which part to amplify is performed by tuning motorized translation and rotation stages. The signal from the output of first OPA is used as a seed for the power amplifier – second OPA stage. The tuning of OPA output wavelength is performed by adjusting crystal angles and time delay between pump and seed pulses.

OPA performance: OPA performances have been tested using a standard PHAROS laser source producing ~ 300 fs pulses at 6 W average power. In order to test OPA at lowest energy limits the laser was operated at 100 kHz repetition rate, that gives 60 **μ**J per pulse. The tuning range is limited by the long-wave transparency limit of BBO crystal that is around 3 μm. The tuneability limit for signal wavelength is governed by the relationship $1/\lambda_p = 1/\lambda_s + 1/\lambda_i$, where **λ**p is the pump wavelength (515 nm), **λ**s is the signal wavelength, and **λ**i the idler wavelength. Therefore, the lowest possible wavelength of the signal wave is around 620 nm. The maximum signal pulse energy is obtained at ~ 650 nm and is of ~ 20% when calculating the ratio of signal to pump pulse (515 nm) energies.

OPA output conversion to UV: OPA output wavelength tuning range can be extended with additional frequency conversion stages, for example by frequency doubling the signal and idler waves. In this way the tunable wavelength range has been extended into the ultraviolet down to 315 nm; the efficiency of the signal wave conversion to its second harmonic is 35%, for the idler wave; this value decreases to 25% for the longer wavelengths (around 1250 nm). The wavelength range can be further extended into ultraviolet by generating the fourth harmonic of the signal and idler waves, and wavelengths down to 210 nm can be achieved, limited by the properties of the BBO nonlinear crystal. Efficiency, measured as the power ratio of the fourth harmonic radiation to the second harmonic

radiation, varies from 5% to 23 % for the signal wave and from 10% up to 40% for the idler wave. Such a high variation of conversion efficiency is limited by the properties of BBO crystal at shorter wavelength: in range < 230 nm of FHS, effective non-linear coefficient of BBO crystal decreases sharply. On the other hand, efficiency of the generation of fourth harmonic of idler wave is lower for wavelengths > 330 nm because of lower pulse energy generated in previous harmonic leading to unsaturated generation of higher harmonic using one crystal for the range.

Once assessed the technical points discussed above, the main goal of second period of Atlas project was the development and implementation of dedicated laser system delivering two synchronized pulses at two different wavelengths in UV region from two independent channels. This part consisted of: a) development femtosecond diode laser pumped Yb:KGW laser system operating at different repetition rates and providing generation of high spatio-temporal quality pulses at 1030 nm with energy up to 1.3 mJ; b) development of module for different harmonic pulse generation at 515 nm, 314 nm and 257 nm; c) development of femtosecond parametric light amplifier (OPA) and harmonic generators based pulse source delivering femtosecond pulses continuously tunable in 210-2600 nm wavelength range; d) full system installation at premises of Università degli Studi di Napoli Federico II. The schematic diagram of the dedicated two channels laser system that was installed in Naples is presented in Figure 1.

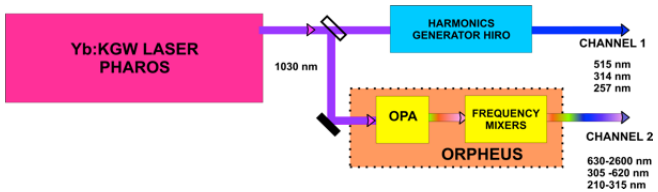

Fig. 1: *Two channel femtosecond UV pulse source.*

Versatile laser system for pumping of frequency convertors: In the frame of the ATLAS project on the base of the technologies and design principles worked out in Light Conversion the dedicated Yb:KGW laser system PHAROS optimized for its effective application in the research on UV-laser photo-induced cross-linking has been developed. The laser is designed using principle of chirped pulse amplification and is manufactured as a single unit comprising of fs pulse oscillator, regenerative amplifier, pulse stretcher-compressor. The compact and robust opto-mechanical laser design includes easy to replace modules (oscillator, amplifier, stretcher/compressor, electronic modules) with temperature stabilized and sealed housings ensuring stable laser operation within varying environments. The oscillator (OSC) produces a train femtosecond pulses that are used as seed for regenerative amplifier (RA). A series of experimental tests and design innovations related to improving of OSC operational characteristics (starting of modelocking, long term stability, OSC cavity dispersion control by implementation of chirped mirrors) has been accomplished. The output OSC oscillator produces the femtosecond pulses and exhibits smooth ~18 nm FWHM spectrum, that corresponds to ~ 80 fs pulsewidth. Average OSC output power is ~1 W power and long-term pulse energy stability is better than 5%. One of the main objectives in laser development was an enhancement of laser output energies. Another characteristic of high importance is a laser ability to operate at

different repetitionrates maintaining low values of energy variations for long periods of time. Improvement has been achieved by careful RA cavity design, implementation of computer controlled cooling of RA frame and "power lock" function in pump module driver operation.

The maximum pulse energy of 1.3 mJ is produced at repetition rates of ≤ 2 kHz. With increasing repetition rate the average output power rises reaching more than 6 W, at the expense of drop of energy per pulse (to 0.5 mJ at 10 kHz and to ~ 30 μJ at 200 kHz). The stability of laser operation during 15 hours of operation was also evaluated. The change in mean of output pulse power is less than 0.2%. Standard deviation of short term power variation is below 0.5 %. Laser output pulse duration is defined by RA gain bandwidth.

Search for pump conditions and cavity geometry has been performed for realization of broadest amplification bandwidth and providing at the same time the pulse amplification to pulse energies > 1 mJ. Pulse FWHM deduced from of output pulse autocorrelation is 176 fs. At 200 kHz repetition rate the pulse width is around 194 fs. PHAROS pumped harmonics generator usually acts as temporal pulse cleaner and even at highest laser output pulse energy the harmonic pulse has smooth, wings-free profile. The spatial parameters of the laser output beam are rather good. Beam asymmetry is negligible and M^2 parameter for both directions through the range of laser repetition rates from 1 to 200 kHz. Laser system is equipped with pulse picker based on electro-optic Pockels cell (PC). The special PC control functions enabling users for prompt change of irradiation conditions in application experiments have been developed. They allow for: a) selection of every n^{th} pulse from the output train of pulses, b) selection of portion of pulses consisting of n pulses. The laser is equipped with an extensive software package, which ensures its smooth hands-free operation and allows for fast and easy Pharos integration into various processing devices.

Fixed wavelength UV pulse generation by harmonics generators: Harmonics generator is an essential option for femtosecond Yb:KGW laser and gives a possibility to convert infrared laser radiation into VIS and UV range making it as effective tool for a research on UV-laser photo-induced cross-linking. Harmonic generator was designed as single unit "HIRO "allowing for generation of second, third and fourth harmonics of fundamental ~ 1030 nm radiation of Yb:KGW laser. In all the frequency conversion stages the BBO crystals featuring wide transparency and phase matching ranges, large non-linear coefficient, high damage threshold and excellent optical homogeneity of different orientations are employed. The orientations and the length of the crystals are optimized for every particular frequency conversion stage. HIRO unit have a separate output port for each harmonic and is equipped with Output selector, which redirects the internal beams for the generation of appropriate harmonics. The measured UV pulse energies at the output of Chanel 1 of the systems was 325 μJ (at 515 nm), 122 μJ (at 343 nm) and 75 μJ (at 257 nm) when pumped with 625 μJ energy pulses at 1030 nm what corresponds to half of maximum available pump pulse energy.

***Tunable UV pulse generation by OPA and harmonic* generators:** The core element of the 2^{nd} system channel that provides the generation of wavelength tunable UV pulses is the optical parametric amplifier. OPA is designed as a two stage parametric amplifier seeded by white light continuum (WLC) and pumped by SH of ~ 180 fs pulses generated by PHAROS. The generation of tunable UV pulses is achieved by employment of two additional harmonic generation stages which converts the tuning range of signal OPA wave to the UV range. SH generator, continuum generator and OPA stages are integrated in single unit "ORPHEUS". The principal scheme of this module is depicted in Figure 2.

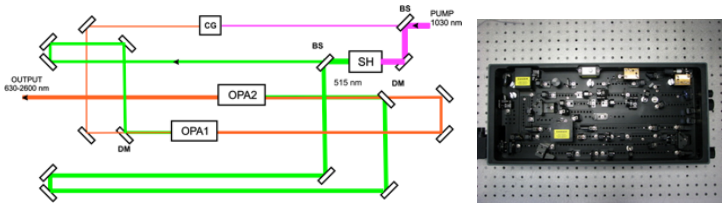

Fig. 2: *Diagram of OPA arrangement and Orpheus outlook.*

A small portion of the incoming pulse is split off and is used to generate WLC in a bulk medium. The rest of the pulse is frequency doubled and used as the pump for two OPA stages. The first OPA stage serves for preamplification of the portion of spectrum of broadband signal coming from continuum generator. The selection of which part to amplify is performed by tuning motorized translation and rotation stages. The signal from the output of first OPA is used as a seed for the power amplifier – second OPA stage. The tuning of the OPA output wavelength is performed by setting of proper angular position of both OPA crystals and adjusting time delay between pump and seed pulses.

Set-up conditions: Parametric amplifiers are pumped by the second harmonic of PHAROS pulses. The SH generator with computer controlled angle adjustment is installed inside ORPHEUS. OPA of ORPHEUS produces the femtosecond pulses tunable in the range of 630-2600 nm. Fresh/residual fundamental and second harmonic radiation (1030 nm and 515 nm respectively) are accessible from dedicated output ports. The tuning curves of ORPHEUS that was installed in laboratory of Università degli Studi di Napoli Federico II has been measured using a pump radiation of 4.2 W of average power at 7 kHz repetition rate. This corresponds to pump pulse energy of 0.6 mJ. The built-in SH generator provided 515 nm pulse generation with up to 55% energy conversion efficiency delivering OPA pump pulse with energy up to 0.33 mJ. The overall tuning range is limited by the long-wave transparency limit of BBO crystal, that is around 2.6 μm. The wavelength of the signal pulses in the three photon parametric interaction is defined by the relationship $1/\lambda_p = 1/\lambda_s + 1/\lambda_i$, where λ_p is the pump wavelength (515 nm), λ_s is the signal wavelength, λ_i is the idler wavelength. Therefore, the lowest possible wavelength of the signal wave when using a pump at 515 nm is around 620 nm. The energy conversion into parametric radiation is most of tuning range is around 20%. The energy content for signal and idler waves is governed by Manley–Rowe relation. The drop of energy conversion in short wavelength region is caused by the rising idler absorption. In the wavelength range close to the degeneracy the lowering of parametric pulse energy is the result of lower continuum signal intensity in this wavelength region. OPA output wavelength tuning range has been extended to short-wavelength visible and UV region by using additional frequency conversion stages. Using SH generator for frequency doubling of OPA signal and idler waves the tuning range of 305-630 nm has been covered with maximum energy conversion efficiency of ~ 38%. The second frequency conversion stage installed at the output of Orpheus ensured generation of femtosecond pulses with wavelengths continuously tunable down to 210 nm.

During first and second period of Atlas project, in parallel with Laser development as discussed above, also the microfluidic device was constructed and tested in order to perform experiment with low amount of material and on selected cell population (see experimental part below).

Setup of the microfluidic system: During the first reporting period of the ATLAS project a first version of the microfluidic system was delivered. The purpose of the first iteration of microfluidic system was to enable testing of UV-fixing strategies. During the first reporting period different fluidic structures were examined with a focus on horizontal fluidic chips (i.e. the laser light is directed perpendicular to the flow). This strategy was judged to provide to short of irradiation time for the cells. During the second period of reporting a new approach to enable longer fixation times was developed. The variant of fixing solutions was termed the vertical flow chip and in this configuration the laser light is guided using mirrors to enable cells to be exposed to the light for a significantly longer period. The system was equipped with system fluids and an automated sample loader. The fluid is pushed through the system using a syringe pump. The control of this first prototype was performed using a PC with dedicated software developed by Sigolis. In the first version of the vertical flow cell a quarts capillary with a relatively small inner diameter (0,25 mm) was selected to enable a small dead volume in the chip. Furthermore the capillary was connected to a holder where also the fluid inlets and outlets were connected. The fluid connectors presented a problem of leaking in the first two versions. This was due to foremost two reasons: 1) The small inner diameter of the capillaries generated a backpressure during high flow rates; 2) The design contained several components that all required correct assembly to enable a proper function. To provide a better functionality, a third iteration assembly was constructed to minimize these two problems. The design is based around a large bore capillary and the coupling interface is fully assembled and glued so that the user does not need to perform any assembly. Furthermore larger bore capillary was used to both enable high flow rates and to enable more light to enter the fluid path. The design uses standard capillaries and it is therefore easy to replace a broken or clogged capillary or to change one with different ID. The final design of the vertical flow capillary has during testing decreased leakage problems.

Association of the microfluidic system with the Laser: Since the complete system is composed by the microfluidic system and the UV-laser, these two needed to be combined to enable full functionality and the microfluidic system was designed to enable coupling through openings in the lid for the fixing cell. To enable alignment of the laser light two independently adjustable UV-grade mirrors were used. The purpose of the design was both to connect incoming light into the capillary but also to couple light out from the UV fixing cell, and thereby enabling measurement of exactly the amount of light that the cells had been exposed to. To reduce risk for light coupling through the capillary, a standard glass capillary was used instead of quarz. An aperture with a smaller diameter that the ID of the capillary in the coupling interfaces also restricts exposer to only the centre part of the capillary. An image of the UV-fixing assembly is illustrated in the Figure 3:

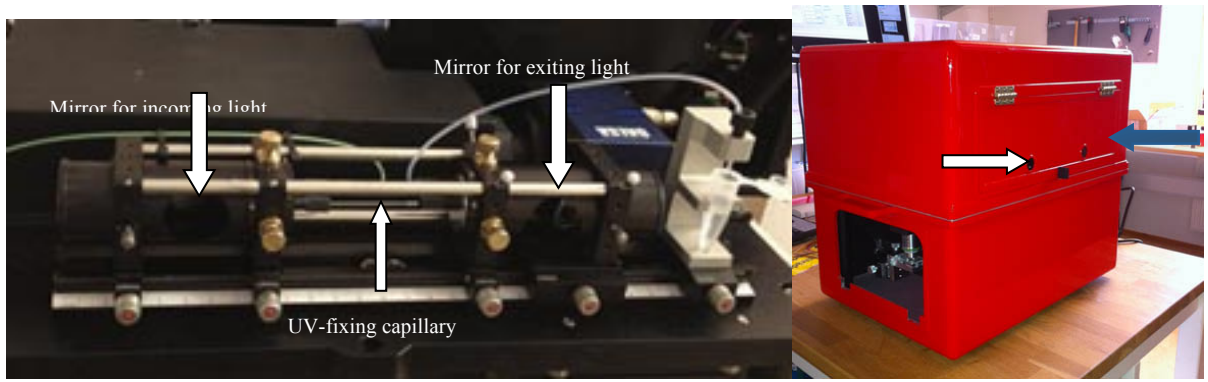

Fig. 3: *Final version of the UV-fixing assembly as mounted in the baseplate of the system. Customized version.*

The image shows the holes in the lid for the UV-fixing cell to enable the UV-laser to be coupled into and out from the system (white and blue-arrow respectively). The open lid exposes the cell sorting chip and detection optics.

Establishment of sorting and cross-link conditions: A goal with the prototype system was also to provide an infrastructure for sorting of cells and this has been the most demanding criteria to meet on a hardware level. During the course of the project several concepts of microfluidic cell sorting has been evaluated, most of where different sorting hardware was tested. The final concept for cell sorting is based upon a dedicated µcontroller that was designed and programmed on low-level by Sigolis. The µcontroller hold a number of commands that can be called upon by Brinels high-level software. The µcontroller continuously monitor the read out of the high-speed line camera (the system holds two line cameras each monitoring the emission in 530 and 650 nm respectively). When a cell enters in the detection zone in the microfluidic chip an increase in signal is registered by the camera. If the signal is above a selected value as set by the software during calibration of the systems it reports a high output that is received by the µcontroller. The µcontroller then operates a set of high-speed piezo-ceramic valves through a high-side switch. The valves are operated in a parallel configuration where one is coupled to the waste channel of the chip (normally open) and the other is coupled to the sorting channel on the chip (normally closed). This configuration responds in the order of 2-3 ms from image registration to valve opening without invention from the software running on the PC. The µcontroller reports no of counted cells back to the high-level software so that the user can select a specific number of sorted cells. A schematic of the sorting principle is described in the Figure 4.

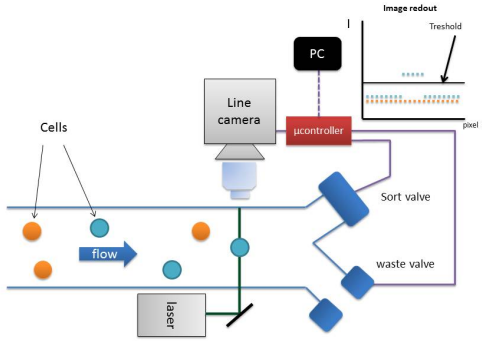

Fig. 4: *Configuration of the sorting part of the prototype system.*

When a cell (orange or blue) passes through the line laser (green) a line based image camera records the signal and real-time analysis is performed between the camera and µcontroller. When a signal above a set threshold value is recorded the µcontroller opens the sorting valve and simultaneously closes the waste valve. The timing of the operation is crucial since the cells move at a rapid pace within the channels. To enable precise control of the sorting a set of optical alignment marks have been incorporated in the last version of the thermoplastic sorting chips. The uses use the on board alignment camera in the system during configuration and select a specific alignment mark used for the experiment. Since the flow speed can be calculated from the flow rate and chip geometries the sorting delay can be set accordingly. To enable fine tuning of sorting performance the system is equipped with a microstage, enabling the user to make fine adjustments of the alignment of the sorting marks in the chip or alternatively set a different sorting delay in the software. This sorting principle has a couple of disadvantages compared to sheet-flow directed sorting regarding speed of sorting, but the design was chosen duet the possibilities to handle lower sample volumes. The final designs of the sorting chips is manufactured by Sigolis using high speed CD-injection molding and the result is a microfluidic CD containing four microfluidic chips with three different canal widths, 50, 150 and 250 µm. The different sizes of channels are to enable optimization of which channel that holds the best balance between sorting performance and time of the analysis, since smaller channels usually enables better sorting performance but also increases time for analysis due to use of lower flow rates.

SCIENTIFIC IDEAS: Chemical principles and the mechanisms of photo-crosslink

Here it is described the determination of the chemical nature of laser-induced DNA-protein cross-linking and the study of alternative mechanisms via photoexcited state and/or radical-induced processes using single and double excitation. Moreover the interest has been focalized on the modulation of the λ max for laser irradiation to fine-tune the photocross-linking optimization and specificity. Another important parameter kept into consideration has been the recognition of the effects of specific DNA/protein molecular processes on the photocross-linking efficiency. In more detail laser induces crosslinking in four

cases: T + His, T + Trp, C + His, and C + Trp, at least at this first experiment sample conditions and laser setup, showing T combinations much better yield than the C counterparts. Except for the whole adduct T + Trp, the signal of which is very clear, the remaining proposed structures for laser irradiation products are not well established yet, and further structural analysis would be required. Analyses by HPLC/MS/MS strongly suggest that some laser-induced reactivity are taking place, at least in the CH, CW and TH cases. Small masses of significant signals corresponding to MS fragmentations have not been possible to trace to the original compound for a variety of reasons. HPLC separation at corresponding retention times and subsequent RMN spectroscopic structure determination are planned, as the better way to identify the actual compound generating MS signal. Despite that, starting from the expected cross-linking product, some MS fragmentation hypothesis can be considered for CH and TH, which explains easily the 553 Da peaks. A first approach to study the influence of "proximity effects" on the efficiency of the cross-coupling has focused on a model system with the reactive group of an aminoacid (tyrosine) covalently-bound to a base (uracil). Two positional isomers have been constructed, with the phenol group attached to the C5 and C6 positions of the base. The photochemical behavior of these compounds is being currently studied both under laser irradiation and under UV light (254 nm) irradiation. The vertical excitation energies and the potential energy surface relaxation processes for 5-benzyluracil system have been studied by partner #8. The results show that there are two relaxation directions, one of which involves geometry changes in the benzene fragment, while in the second case the uracil fragment shows different distorted geometries. As long as, the relaxation process can occur spontaneously in the benzene direction, at the uracil branch this could be initiated only if the C=O bond is vibrationally excited. These studies will be complemented with the CASPT2 / MRCI calculations of both systems, which include dynamic electron correlation and is in progress. The four deoxyribonucleosides have been converted into their corresponding cyclic disiloxanes (1-4) in order to avoid potential reactions of the hydroxyl groups. In order to check the laser induced cross-linking and compare this technique with the classic UV irradiation induced photochemistry, two model molecules, 6-(3-hydroxybenzyl)-uracil and 5-(2-hydroxybenzyl)-uracil, were synthesized. The synthesis of the first isomer (Scheme 1) was achieved. Namely, the use of microwave irradiation for the condensation of the β−ketoester 3 and urea 4 to furnish 5 allowed us to afford the desired product 6 with substantially improved yield (three times the value previously reported in the literature).

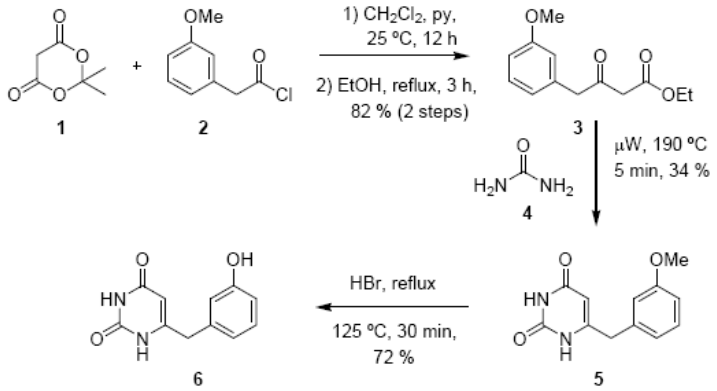

***Scheme 1**: Improved synthetic route to 6-(3-hydroxybenzyl)-uracil.*

The synthesis of 5-(2-hydroxybenzyl)-uracil (9) requires just one step (Scheme 2) that involves a Friedel-Crafts reaction between phenol (8) and 5-methyluracil (7).

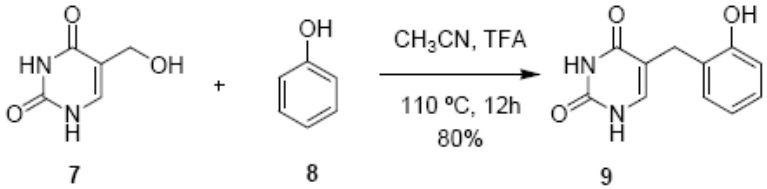

***Scheme 2:** Optimized synthetic route to achieve 5-(2-hydroxybenzyl)-uracil.*

The first ATLAS-WP2 laser induced cross-linking experiment (L01) was performed. Four bases (B), ten amino acids (aa), and the combinations between them were tested.
Table 1 summarizes the samples used for this experiment.

Table1.

1	2 a in d1	3 b in d1	4 c in d1	5 d in d1	6 e in d1	7 f in d1 **from 2 to 1 ml**	8 g in d1 **evap.**	9 h in d1
10 1 in d1	11 1+a in d1	12 1+b in d1	13 1+c in d1	14 1+d in d1	15 1+e in d1	16 1+f in d1	17 1+g in d1 **evap.**	18 1+h in d1
19 **evap.** 2 in d2 +MeOH	20 2+a in d2 +MeOH	21 **evap.** 2+b in d2 +MeOH	22 2+c in d2 +MeOH	23 **evap.** 2+d in d2 +MeOH	24 **evap.** 2+e in d2 +MeOH	25 **evap.** 2+f in d2 +MeOH	26 **evap.** 2+g in d2 +MeOH	27 **evap.** 2+h in d2 +MeOH
28 3 in d1 +MeOH	29 3+a in d1 +MeOH	30 3+b in d1 +MeOH	31 3+c in d1 +MeOH	32 3+d in d1 +MeOH	33 3+e in d1 +MeOH	34 3+f in d1 +MeOH	35 **evap.** 3+g in d1 +MeOH	36 3+h in d1 +MeOH
37 4 in d1	38 4+a in d1	39 4+b in d1	40 4+c ind 1	41 4+d in d1	42 4+e in d1 **from 2 to 1 ml**	43 4+f in d1	44 4+g in d1 **evap.**	45 4+h in d1
46	47	48	49	50	51	52	53	54
55	56 i in d1	57 1+i in d1	58 **evap.** 2+i in d2 +MeOH	59 **time=33 sec** 3+i in d1 +MeOH	60 4+i in d1	61	62	63
64	65 j in d1 **evap.**	66 1+j in d1 **evap.**	67 **evap.** 2+j in d2 +MeOH	68 **evap.** 3+j in d1 +MeOH	69 **evap.** 4+j in d1 **evap.**	70	71	72
73	74	75	76	77	78	79	80	81

Samples were prepared at Vigo laboratories and a sample of each vial was sent to Napoli for laser irradiation. The remaining solutions were stored at -30 ºC. When irradiated, samples returned to Vigo, high performance liquid chromatography (HPLC) separation followed by mass spectrometry (MS) and ultraviolet spectroscopy (UV) measurements were performed for both irradiated and non-irradiated samples allowing us to compare them and probe the cross-linking for each combination. The MS measurement protocol is schematically depicted in Figure 5. In the HPLC column, separations were performed using the following setup: 1mL/min pump rate; H2O/CH3CN mixture as eluent, with a smooth gradient during 29 minutes from 95/5 to 0/100, and then again a 1 min washing phase at starting 95/5 composition.

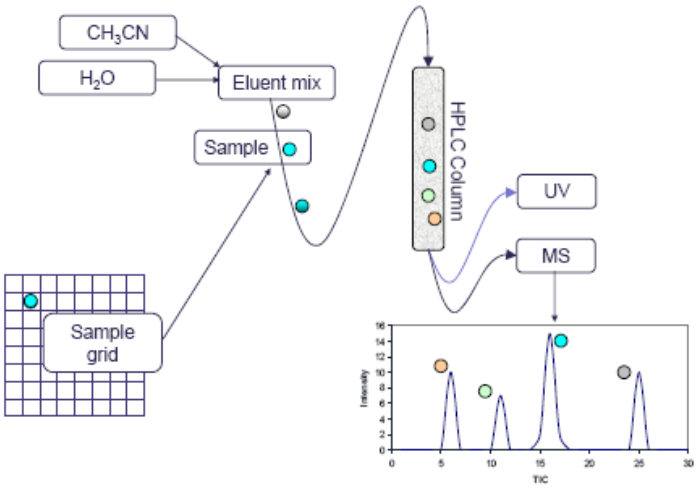

Fig. 5: *Processing and detection protocol. The sample is carried through the system by an eluent mixture consisting of variable proportions of water and CH3CN. A reverse-phase HPLC column separates the compounds of the mixture depending on their hydrophobicity and polar nature, and then the separated products are splitted along two parallel channels to UV and MS detectors. In MS detector, separation products are vaporized and ionized using electrospray ionization (ESI).*

This experiment was aimed to establish the systems that appear sensitive to laser activation; therefore we had to start searching across the whole MS data set in order to obtain evidences, and then analyze in more depth the positive cases. The expected masses of amino acids, bases and the corresponding adducts are shown in Table 2.

		B-10 (1)	B-19 (2)	B-28 (3)	B-37 (4)
	Pm_T	**493.25**	**509.25**	**469.24**	**484.24**
aa-2 (a)	**269.14**	762.39	778.39	738.38	753.38
aa-3 (b)	**260.17**	753.42	769.42	729.41	744.41
aa-4 (c)	**318.16**	811.41	827.41	787.40	802.40
aa-5 (d)	**235.09**	728.34	744.34	704.33	719.33
aa-6 (e)	**219.11**	712.36	728.36	688.35	703.35
aa-7 (f)	**279.15**	772.40	788.40	748.39	763.39
aa-8 (g)	**232.11**	725.36	741.36	701.35	716.35
aa-9 (h)	**323.35**	816.60	832.60	792.59	807.59
aa-56 (i)	**295.14**	788.39	804.39	764.38	779.38
aa-65 (j)	**274.16**	767.41	783.41	743.40	758.40

Table 2*: Expected mass values. In boldface are shown amino acids and bases, while in plain text are shown the values corresponding to simple adducts of the bases at the top column and amino acid at the left row.*

Additionally, loss of several fragments has been taken into account, namely -Me, -tBu, -COOMe, and –Boc, and the corresponding signals were found in the spectra depending on the case. For example, Figure 6 shows peak structure of Phe in 1-f binary combination (grid number: 16) after irradiation. At the retention time this spectrum was recorded, and no strong signals other than Phe ones are present.

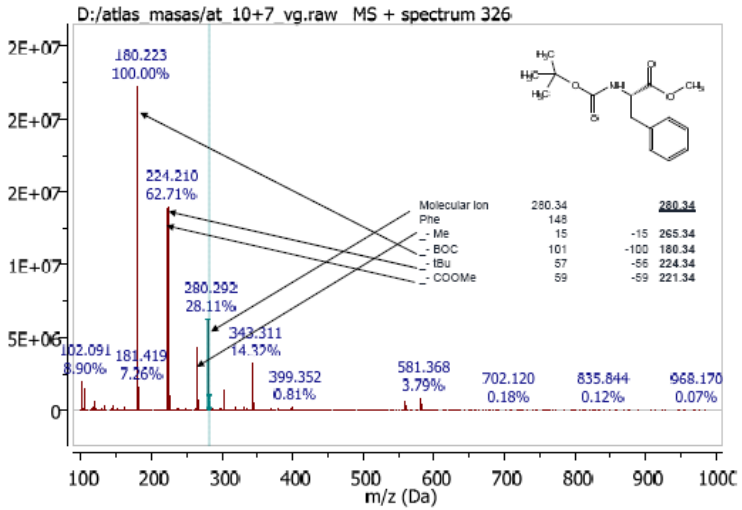

Fig. 6: *Phe mass spectrum main signals, along with assigned fragments, for the laser irradiated A + Phe binary combination (1-f , grid number: 16). Considering both, peak fine structure (isotope dependent) and group of signals like these, which are characteristics of each molecule, we are able to identify separation products. If preparation and processing protocols were strict, the identification could be even quantitative.*

Two basis, adenosine (2'-deoxyadenosine-TIPS, A) and thymidine (2'-deoxythymidine-TIPS, T), were analyzed first, resulting in no cross linking for binary combinations of amino acids with A, and at least one clear adduct for T. The cyclic structure (purine) of A is similar to guanosine (2'-deoxyguanosine-TIPS, G), and T (pyrimidine) to cytidine (2'-deoxycytidine-TIPS, C); no further analysis was performed with G, and for C we have considered only the corresponding positive T cases. Irradiated samples intensities are, in general, greater than those of the non-irradiated counterparts, due probably to solvent partial evaporation. Bases and amino acids retention times are well reproduced across the whole series of samples. Additional signals of irradiated reactive combinations are found at retention times between those of the basis and amino acids, with few exceptions of very low intensity. Although only the main signal of each spectrum/molecule is shown in Table 3, typical ESI fragmentation was taken into account for analyzing non only amino acids and bases, but adducts or hypothetical molecules corresponding to new signals. In T cases, T retention time is exactly the same across all the irradiated and non-irradiated combinations (not only those shown here) and varies slightly with respect to the base alone. T combinations with His and Trp show reactivity when exposed to UV laser irradiation, the first one giving a new signal of 553 Da and the second one giving another one of 803 Da, equal to the expected whole adduct, the only one detected. Proposed products for these values are shown in Figure 7.

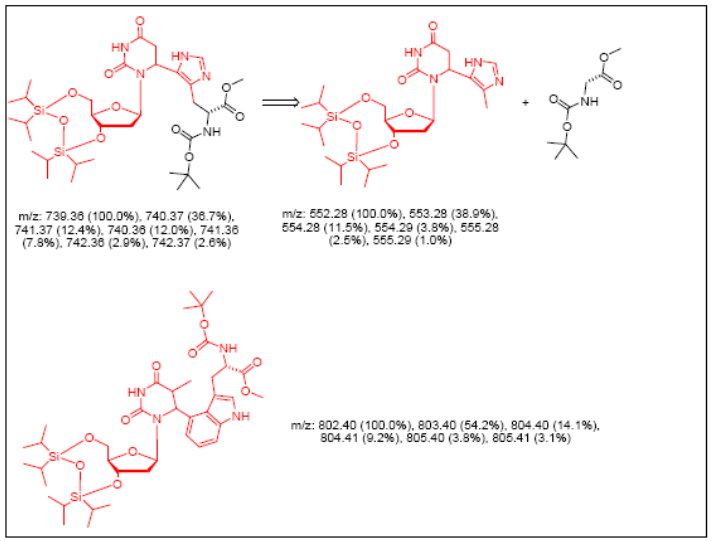

Fig. 7: *Proposed structures for the irradiation product in the cases T + His (top) and T + Trp (bottom). The first would be an adduct fragment, and the second the whole adduct.*

Combination T + Asp shows a strange variation in the intensity of the 808 Da signal, which corresponds to the adduct T + Asp + Me. The laser influence results in lowering the intensity of the signal, so the simple explanation is that the laser is not forming but instead breaking the adduct.

Note that the 808 Da signal is varying form 1 (x10^{6}, factor omitted in the following) to 0.31 while T signal is increasing from 0.18 to 3.15, and Asp signal from 11.53 to 53.17, therefore relative variations are much more important that can be apparent from the 808 Da signal alone: 15.71 times smaller for the adduct and 3.59 times greater for the base after irradiation, with respect to amino acid intensity sample preparation too. As an example, in the combination T + Cys, the signal ratio [469 Da]/[263 Da] reduces from 1.08 to 0.31, being 469 Da and 263 Da the masses of Cys-Cys dimer and Cys amino acid respectively. As a general behaviour, C signal is wider across the retention time in irradiated samples, since transformation of the base at some extent is expected, although the molecular peak is detected at similar retention times in both non irradiated and irradiated samples. Some reactivities are detected in C + His and C + Trp mixtures. Nevertheless, intensity values are considerably lower than in T + His and C + Trp mixtures, particularly when relative ones are considered. In the irradiated samples, adduct molecular ion signal is not detected, but instead additional peaks at different masses. C + His shows a peak at 553 Da, the same mass of the T + His product. Peak structure analysis reveals some differences between them: m/z (T+His) = 553.339 (100.00%), 554.410 (20.77%); m/z (C+His) = 553.276 (100.00%), 554.221 (38.17%), 55. A second ATLAS laser induced crosslinking experiment (L02) was performed. Being the protocol a refined and consolidated version of the used for the first one (L01), we will focus in the few differences to be mentioned. This time, after some observations, sample stability at room

temperature was confirmed. Hence, all samples were prepared at Vigo, stored, sent to Napoli, irradiated, sent back to Vigo, and analyzed at room temperature. The maximum estimated variation being 30ºC during all the process. From the first laser experiment (L01) four positives were considered, corresponding to the T and C DNA bases combined with His and Trp amino acids. We design these four combinations as CH, CW, TH and TW, using the standard one letter code for each compound. Only the selected four compounds and the four corresponding combinations were prepared at Vigo laboratories. A box containing the resulting eight vials (Fig. 8) was then sent to Napoli for laser irradiation. A whole array of laser setups was proposed in order to a) confirm the L01 suggested reactivity and b) establish the laser intensity dependent and exposure time dependent behavior.

	T	C
W	T+W	C+W
H	T+H	C+H

	10	10
10	32	32
10	32	32

Fig. 8: *Vials sent to Napoli. The left part describes the compounds and in the right part the corresponding volumes in mL are shown. Concentration was 0.01 mol L-1 in each component, being the total concentration 0.01 mol L-1 for the pure substances and 0.02 mol L-1 for the binary mixtures.*

For each binary mixture, five laser intensities and three exposure times were considered. Irradiation was performed in three sessions, and some setup changes had to be incorporated in the last one, due to the laser status. All the samples were irradiated according to the corresponding setup, and sent back to Vigo, where HPLC-MS analysis was performed (Table 3). Just before each irradiation, sample of 1 mL was taken from the corresponding vial and put in the laser cell, and just after irradiation, the sample was moved to a 1.5 mL microcentrifuge tube and placed in an isolated box for later sending back to Vigo.

labels			laser setup		
				irrad.	
HPLC	*comp.*	*laser*	*intensity* [10E-6 J]	*time* [s]	*spot size*
97	CH	nc	none		
98	CW	nc	none		
99	TH	nc	none		
100	TW	nc	none		

Table 3: *Set-up of the irradiation samples in the experiment. Headers, from left to right: HPLC-MS sample code, compounds in the mixture, laser sample code, laser intensity, laser exposure time, and spot size. The null control samples (nc) were not irradiated at all, but included in the box to check the effect of travel.*

The 5-benzyluracil (5BU) system is build by two molecular fragments of benzene and uracil linked by CH2 bridge which is connected to the uracil at the C5 atomic position. The geometry structure of 5BU is presented in Figure 9.

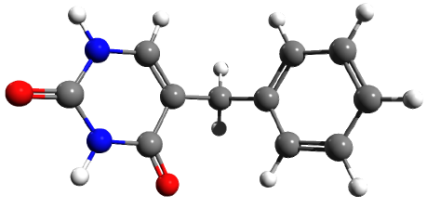

Fig. 9: *The geometry structure of 5BU.*

The vertical excitation spectra of 5-Benzyluracil and 6-Benzyluracil (6BU) have been obtained using the time dependent density functional theory (TDDFT) with cc-pVTZ triple ζ basis set, method which is implemented in the Gaussian 03 quantum chemical program. The results were analyzed using the Gabedit molecular graphics program and the theoretical absorption spectrum is presented in Figure 10. As we can observe there are significant differences between the absorption spectra of 5BU and 6BU systems. While in case of 6BU, the first excited state has a very small oscillator strength and implicitly poor absorption of the radiation, for the 5BU system in case of the first (S1) excited state we have considerable strength of absorption.

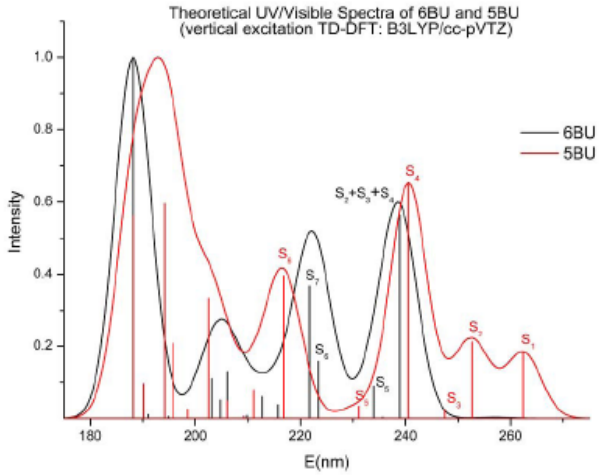

Fig.10: *The theoretical UV/Visible absorption spectra for 5-benzyluracil (red line) and 6-benzyluracil (black line).*

On the other hand, the second (S2), third (S3) and fourth (S4) excited states of 6BU are degenerated (having near the same excitation energy levels), while in the case of 5BU they are very well separated between them. Knowing the lack of the TDDFT method near the degenerated states we should mention that this energy level degeneration must be investigated also by multi-reference (MR) method, like multi-configuration self-consistent field methods (MCSCF). This major difference can be exploited in order to obtain the desired selectivity in exciting these molecular systems. Having the CH2-bridge between the uracil and benzene fragments an internal rotation around the C-C single bonds can easily occur. Therefore, we have investigated the effects of internal rotations on different excited states of 5BU. In Figure 11 we present the dependency of the oscillator strength in function of the excitation wavelength and the internal rotational angle for both S1 and S2 states of 5BU. The S1 state is an n→π* transition, while the S2 excited state correspond to the π→π* transition. One can observe that due to the internal rotation the absorption line will be enlarged and we obtain a line width with two domains: 259–265 nm and 269–272 nm both for both S1 and S2 states. The intensity of the oscillator strength is also depends on the rotation angle and we can see that in both cases the highest intensity does not coincide with the oscillator strength of the equilibrium position.

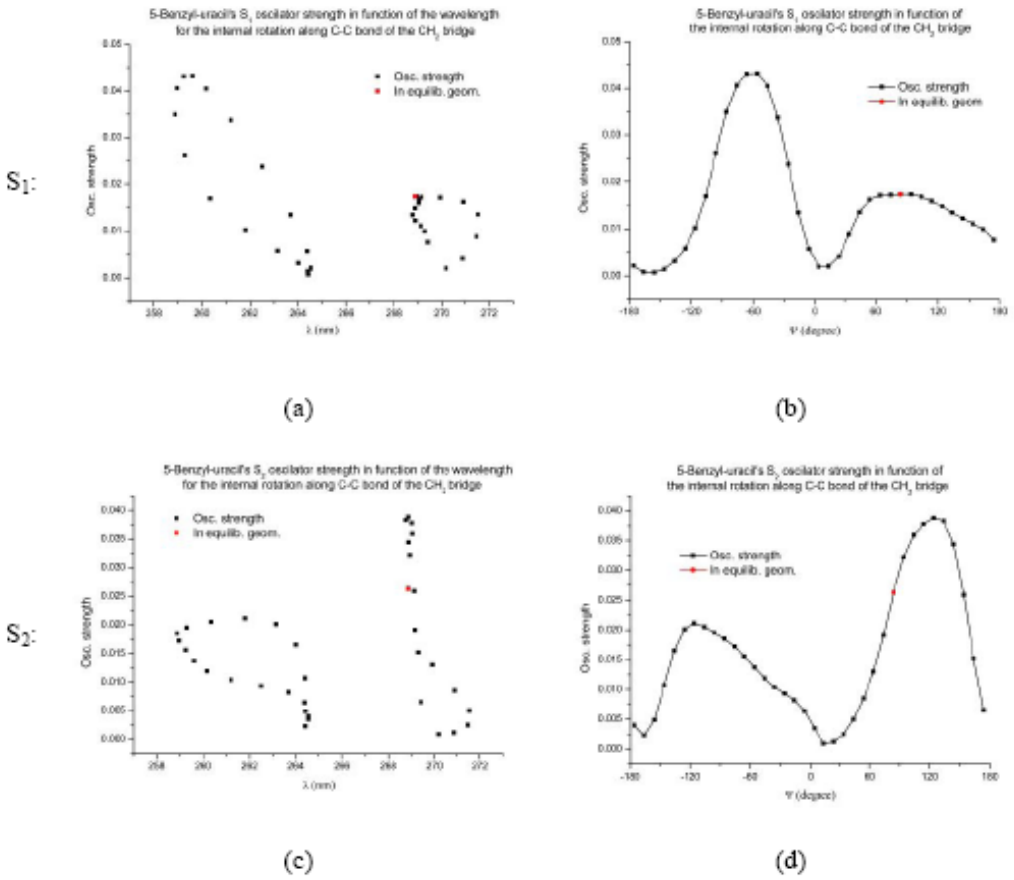

Fig. 11: *Dependency of the oscillator strength in function of the excitation wavelength and the internal rotational angle for both S1 and S2 states of 5BU.*

Due to the fact that the TDDFT method is not a multireference theory, this does not always give correct results near the energy degeneracy (called also static correlation effect). For this reason the vertical excitation energies were also computed using the state-averaged complete active space self-consistent field method (SA-CASSCF) which is a special case of the MCSCF theory. Exploring the relaxation pathways of excited states along the potential energy surface (PES) is very important in order to understand the properties and dynamics of the excited states. The geometry optimization of first and second excited states of 5BU was performed considering the SA-CASSCF method, implemented in the Molpro program package. For these calculations the DZP basis set was used. In our active space were included 10 double occupied orbitals and 14 states. For the initial geometry, the ground state (S0) equilibrium configuration was used. Starting the first (S1) or the second (S2) excited state optimization, the relaxation process always fell in the benzene domain. For the S1 state the optimized geometry could be easily found after a few optimization cycles. The optimized geometry of S1 does not differ so much from the S0 ground state geometry, only the C-C bonds of the aromatic ring show a little bit longer bond lengths (0.2–0.3 Å). The optimized S1 energy is at 4.63 eV higher from the S0, but is with 0.22 eV lower that the S1 vertical state. This relaxation process is qualitatively similar with the simple benzene ring relaxation. In case of S2 states we weren't able to find a stable geometry structure before to reach the conical intersection (CI) point between S1 and S2 states. In Figure 12 we present the S1 optimized structure and the geometry at the CI point.

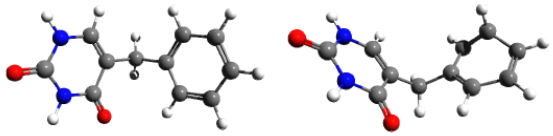

Fig. 12: *The S1 equilibrium structure and the geometry at the S1S2 CI point.*

As we can see on the second picture of Figure 12, for the S1S2 CI point the aromatic ring of the benzene fragment is highly distorted which is also confirmed by the relatively high energy value (6.49 eV) compared to the ground state. Another interesting case would be the conical intersection point between the S0 and S1 states, which is still under our investigation. In this way we would be able to draw comprehensive conclusions about the dynamics of the relaxation processes which could occur in the benzene branch of the 5BU. In order to study the relaxation process in the uracil region, the starting geometries were carefully chosen. In general, we followed the uracil relaxation scheme, where in the ground state geometry structure the C=O bond distance was stretched. In this way the relaxation process were initiated on the uracil branch, while the benzene ring geometry remains as it was obtained in the ground state case. Here, we found two different equilibrium geometries S2_A and S2_B structures (see Figure 13), having 5.99 eV and 6.46 eV energy differences, respectively, from the S0 level.

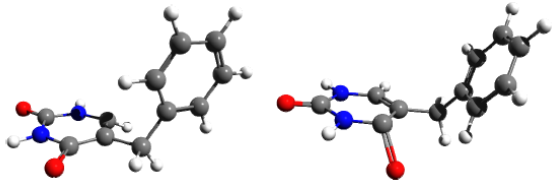

Fig. 13: *The S2_A and S2_B equilibrium geometry structures of 5BU.*

In the *A* case the uracil geometry is totally distorted, one of the C=O bond is stretched and becomes near a single bond. Due to this effect the bond between C4 and C5 becomes a double bond, while the C5–C6 double bond is changed to single bond. In the *B* case only a C=O bond will come out from the uracil plane and its bond length is changed from the double bond to weaker than a single one (dC-O = 1.63 Å). The initial configuration for S1 excited state which might show geometry changes also at the uracil branch was started considering the S2_A geometry. In our opinion this geometry is quite general, having non-planar structures. After a few optimization cycles we have obtained the S1 geometry which topologically is similar with the S2_A optimized structure, differs only in some bond distances (see Figure 13). The energy minimum can be found at 4.19 eV over the ground state energy. Two another calculation are in progress, one of them is the CI_S1S2 conical intersection localization, while the other one is the intersystem crossing point between S0 singlet and T0 triplet states. Having these geometries we will be able to draw up a scheme of the relaxation process both at the uracil and benzene branches. A hypothetic scheme which is based on the results up to now is shown in Figure 14.

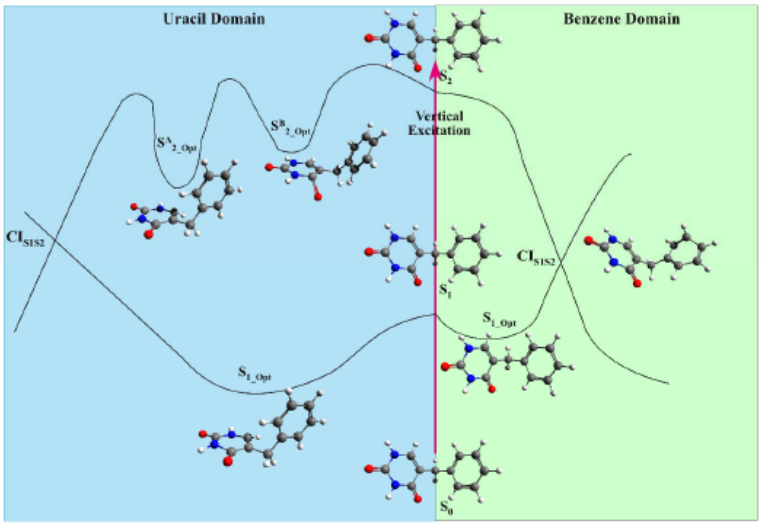

Fig.14: *The schematic picture of different excited energy states for 5BU.*

The structural models to test the possible laser-induced interaction between DNA and proteins were selected as follows: first, the side chain of the aminoacids (aa), with the required protecting groups in the amino and carboxylic acid functional groups of each aa, emulate the proteins; second, each of the DNA nucleosides with a triisopropylsilyl (TIPS) as protecting group of the alcohol moieties, emulate the DNA.
From the experiments carried out with the combinations of protected aa with protected nucleic acid bases, we could conclude that the photo cross-linking laser irradiation is more efficient with the aromatic aminoacids, in particular the paired combinations between Histidine (H) and Tryptophan (W) with Cytosine (C) and Thymine (T). From a subsequent experiment with these mixtures, the combinations CH, TH and CW were found to be the most suitable for the photo cross-linking induced by laser irradiation. Therefore, we focused on these motifs as structural models for subsequently study the proximity effects of aa and DNA bases. The only aa-nucleic base chimera synthesized is the one depicted in Figure 15. It is a derivative of uracil and the aa histidine connected via an amide bond. However, despite our efforts we could not purify the final product. Therefore no irradiation experiments, at the laser optimized conditions, were conducted.

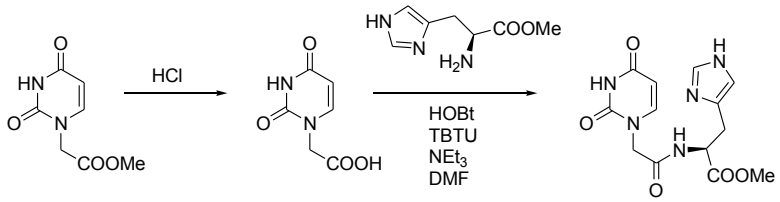

Fig. 15: *Acidic hydrolysis of methyl 2-uracilacetate and amidation of the carboxylic acid with protected histidine.*

NIRDIMT attempted to model first the laser interaction with a molecular system of interest in this project. A model system with a single optically active electronic state in contact with a dissipative environment (bath), which can be a solvent or the strongly coupled intramolecular modes was described first, together with the numerical implementation. However the lack of information concerning the strength of the coupling system-bath parameters makes the system hard to apply for our cases of interest. As a second approach a real molecular system (5-benzyl-uracil) and its interaction with a laser field in the framework of the time-dependent Kohn-Sham formalism was selected, using the B3LYP exchange-correlation functional and cc-pVTZ bases set to describe the electronic structure of 5-benzyl-uracil. However, we must take into consideration not only the conformations of the initial molecule when the excitation process occurs, but also all the minimal conformations that have an independent weight in the global statistical distribution in solution. Therefore the excitation process must start from each of the selected conformations. For that purpose we studied the PES of the possible conformations in solution varying the torsional angle of the two connected rings in both directions (uracil → benzene and benzene → uracil) for both model systems, at the PM3 level of theory, and the results are shown in Figure16.

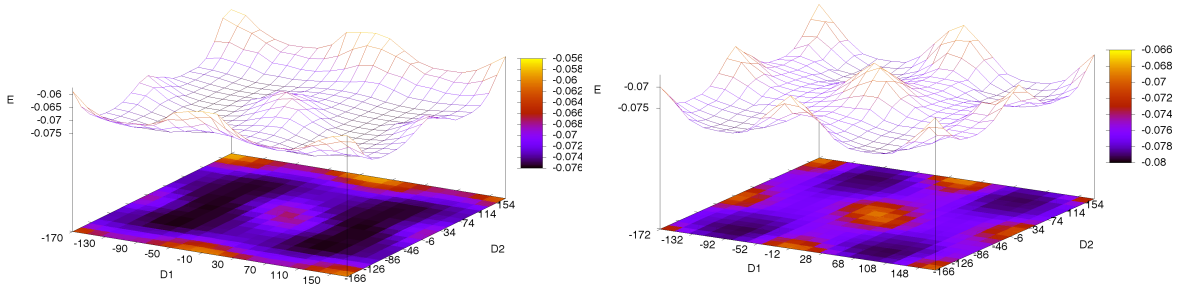

Fig. 16*: Bidimensional scan of the two torsional angles of the carbon linking the two rings in both directions of 5- and 6-benzyluracil.*

5-benzyluracil has two very loosing potential wells in which a fine structure of 3 minima could be seen. Therefore, a total of six conformations, which are mostly degenerated, must be taken into account in order to study the population of the excited states. On the other hand, 6-benzyluracil has four iso-energetic minima in the PES, which are symmetric, and then two minima must be globally analyzed in the excitation process. TDDFT calculation of all these structures has been carried out to determine the vertical excitation process and the global weight of each conformation in the photo-induced transformation. On the other hand we have conducted laser and traditional UV irradiation experiments on the samples shown in Figure 17. Irradiation with a UV-lamp led virtually to the same results previously reported after 16 hours of irradiation. Indeed, by increasing the irradiation time the yields could be improved. The irradiation of the samples by the laser apparatus demonstrated that within 30 minutes of irradiation the results are comparable to the previous ones. We conclude that the laser facilitates the photocross-linking process accelerated by the pulse of energy received and the effectiveness of the absorption of these photons by the molecules.

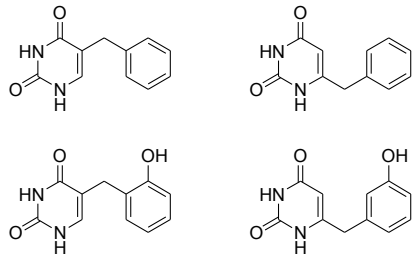

Fig. 17: *Synthesized models for uracil with the side chains of phenylalanine and tyrosine, in position 5 and 6 of the uracil respectively, that were subjected to irradiation both with a UV lamp and a laser.*

The mechanistic proposal for the photocross-linking was then evaluated. The excitation energies for the singlets and triplets at the TDDFT (B3LYP) level of energy, shows that only the first two singlets and triplets affect the evolution of the cross-linking process after the absorption of a photon of the appropriate energy. The remaining excited states have a very high energy, and their implication in the induced reaction between the aminoacid and the nucleic base is minor at better. The evolution of the irradiated 5-BU is depicted in Figure 18, which depicts only the calculations with the singlets in both the uracil and the benzene ring domains, separated by the methylene group. The evolution of the system through the capture of the ion radicals generated in the excitation process of the molecule is not possible. The only path to release the energy absorbed with the photon is the fluorescence process or the decay from the S1 or S2 excited states, depending on the energy of the absorbed photon. From S2, the more feasible deactivation mechanism appears to be the radiationless decay to the minima in the uracil domain and from there a fluorescence emission to the ground state. If the energy is sufficiently high there is a conical intersection that leads to the S1 potential energy surface. Again, the minima on this surface are located in the uracil domain, but there is another conical intersection achievable in the relaxation process that leads to the ground state.

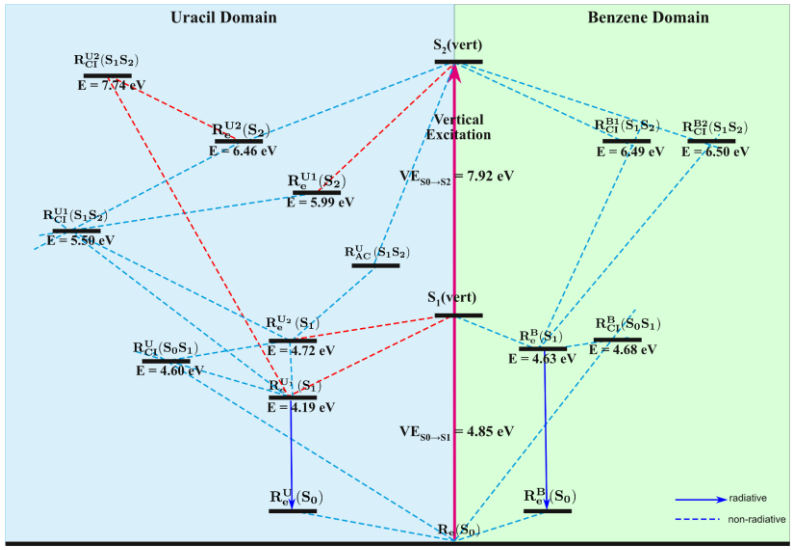

Fig. 18: *Calculated feasible evolution of 5-BU in the excited stated when no evolution of the formed ion radicals could occur. The only pathway is the decay through a radiationless process or a fluorescence mechanism from the S1 or S2 excited states.*

The mechanism proposed for the evolution of the chemical interaction between the aa of the proteins and the nucleic acid basis of the DNA is a radical process initiated by the laser irradiated photon (with the UV absorbance wavelength, thanks to the frequency tunable apparatus) which excites both molecules, generating each radical species that will evolve through their excited states until the reaction between both fragments takes place. In order to support this mechanism we carried out some calculations using 6-benzyluracil as model in the presence of MeOH or even MeOD, simulating the NMR experiments, and MP2 calculation method. A diradical process, in which both parts of the molecule (the aromatic side chain and the nucleic acid base) are excited, with the concomitant formation of a radical anion in one branch of the molecule and a radical cation other branch is proposed. In the ground state, calculations show that the diradical species of 6BU are ~ 80 kcal/mol higher in energy than the singlet ones. Once the di-radical is formed the energy barriers are high enough to render the reaction unfeasible at room temperature. Therefore the reaction must occur in the excited state. Figure 19 shows the reaction profile of the di-radical species until the cross-linking process is achieved. The calculations are not complete yet, since some stationary points are not completely characterized, but it is expected that the bond-formation in the excited state takes place along the proposed reaction coordinate.

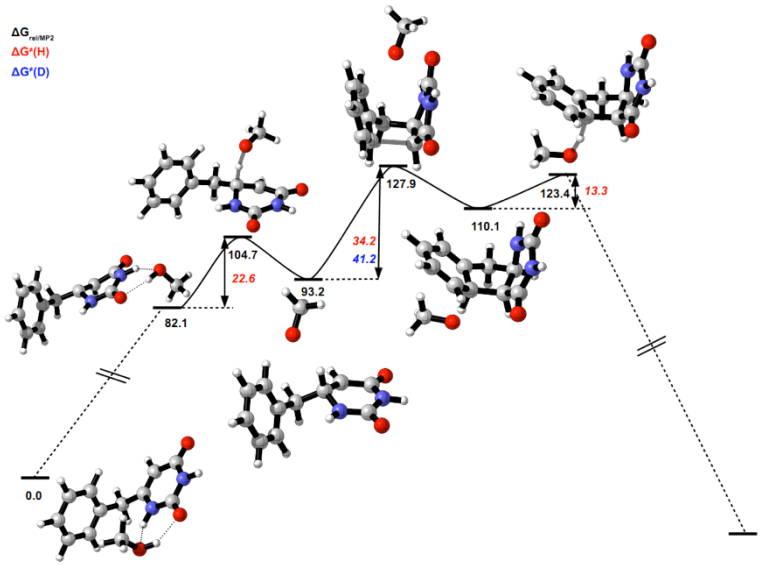

Fig. 19*: Calculated diradical mechanism for the evolution of laser-irradiated 6BU in the presence of MeOH or MeOD, calculated at the MP2/cc-pVDZ level. The energies are given in kcal/mol. The final product and the evolution of the non-radical species as singlets are still under investigation.*

SCIENTIFIC IDEAS: set up and biological application of LChIP

ChIP (Chromatin ImmunoPrecipitation) is an assay that provides direct evidence of crosslink induction between DNA and a regulatory protein. Final goal of Atlas has been the setting out of an alternative tool for crosslinking to test in L-ChIP. The efficiency of L-ChIP was compared with conventional chemically crosslinked ChIP and it has constantly been improved.

In preliminary tests a combination of high-energetic laser parameters (able to promote the bases excitation) were applied to study the crosslink formation but the results from the ChIP assays, for different genomic regions were not comparable to that of the chemical ones (data not shown). To better understand the cellular behavior in response to the laser treatment, several orthogonal methods were applied, looking at cellular viability/mortality, the activation of pathways of DNA damage recognition and repair, the cell cycle progression and the integrity of DNA itself.

The aim was to determine a laser condition by which the energy released to the cells was strong enough to promote the crosslink induction but not too strong to disrupt the DNA or damage it in an irreversible way (and so interfere with the qPCR following L-ChIP experiments). Once understood that, in the used conditions, the DNA inside the cells was damaged and that this damage could interfere with the downstream analysis, the next step (in the process of defining to best conditions for subsequent ChIPs) was to progressively decrease the energy, both for total number of photons and repetition rate.
It is worth stressing a wide window of parameter values have been investigated. When using 257-nm pulses we have tested energy per pulse in the 1-150 μJ range and pulse repetition rates in the 1-50 kHz range. Overall irradiation times have been tested within the 10-300 seconds window.
When using 300-nm pulses two conditions have been tested corresponding to 7μJ – 7 kHz and 7μJ – 2 kHz. Finally, in Table 4, hereafter, the parameter values which leaded to the best signal-to-noise ratio in ChIP analyses to detect photo-induced DNA-protein crosslink are reported.

Pulse energy	**Repetition rate**	**Pulse carrier wavelength**	**Sample irradiation geometry**	**Beam focusing**
7 μJ	2 kHz	257 nm	Cuvette – Capillary (3rd set up)	NO

Table 4: *Summary of the best parameter values/set up conditions for the sake of DNA-protein crosslink maximization together with cell damage and T-T dimer formation minimization.*

This point is also the one for which the DNA damages inside cells are minimized, as reported in Figure 20.

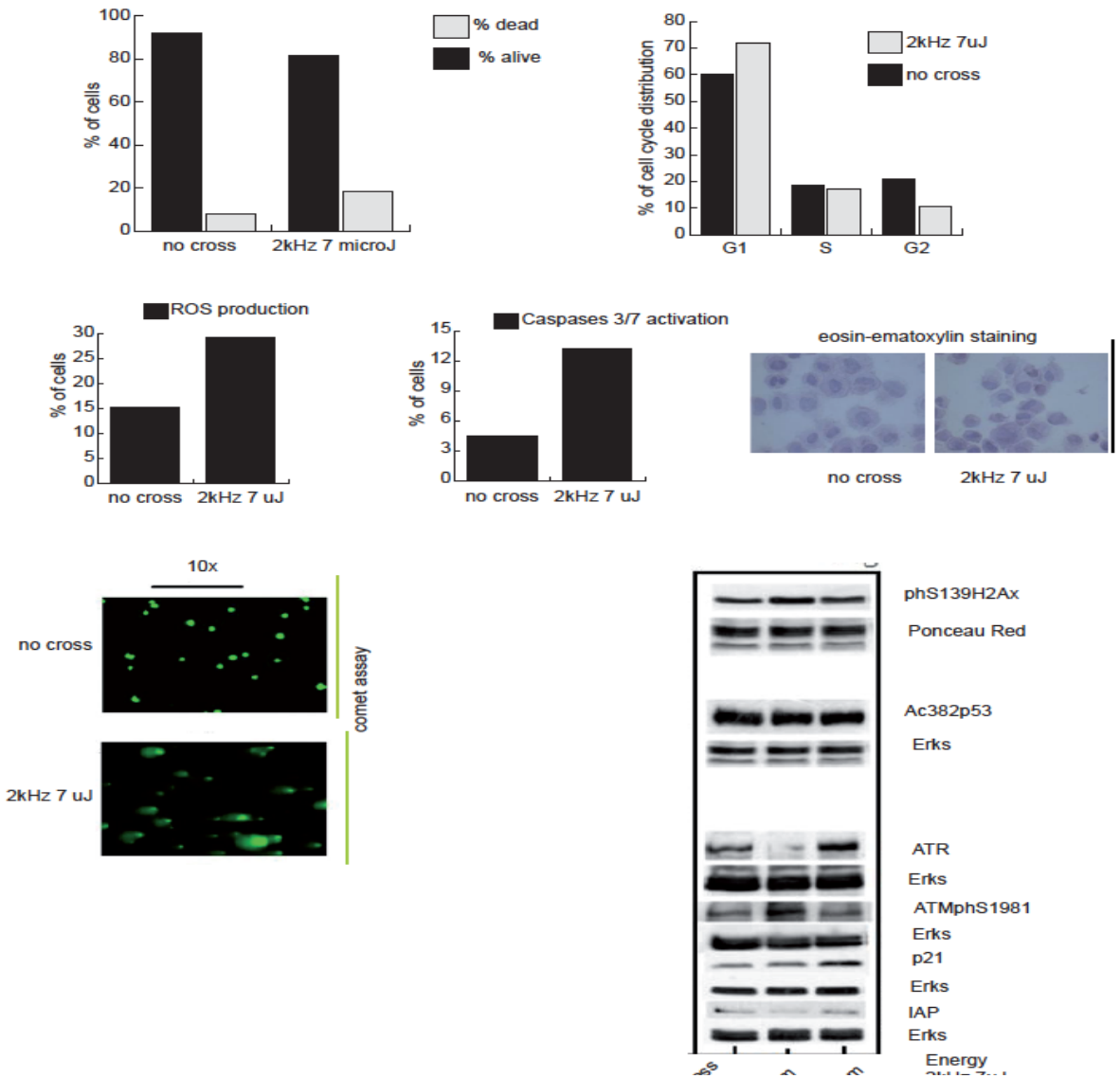

Fig.20: *Data for the cell damages obtained at 7μJ – 2 kHz. Upper left: death and survival percentages; upper right: cell cycle distribution; center left to right: ROS production, caspase assay and Eosin-ematoxylin staining; Bottom left to right: comet assay, western blots of the indicated factors.*

As it is shown, PI incorporation, cell cycle analysis, eosin-ematoxylin staining and comet assay, revealed no significant differences between 7μJ – 2 kHz point and non-treated cells. ROS production and Caspases 3/7 activation are instead increased in the UV-laser treated sample comparing with the control, indicating that pro-apoptotic pathways are however activated. This notion is further corroborated by Western blots, in which some proteins involved in cell death are induced or activated (such as phosphorylated form) when the wavelength of UV light is 260 nm but not when 300 nm is used. In addition, the formation of dimers (detection following the manufacturer's instructions ABNOVA) at 7μJ – 2 kHz 260nm was higher than with 300nm, as reported in Figure 21.

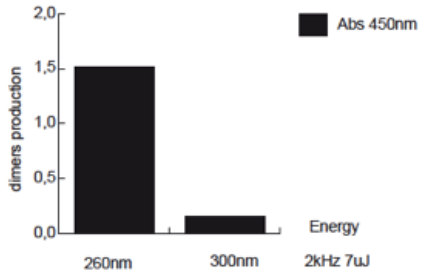

Fig. 21: Pyrimidine dimers production assay at 7μJ – 2 kHz (260nm vs 300nm).

Regarding pyrimidine dimers production, the formation of the two major UV-damage products are a CPD lesion (left) and a (6-4) lesion (right) as shown in Figure 22.

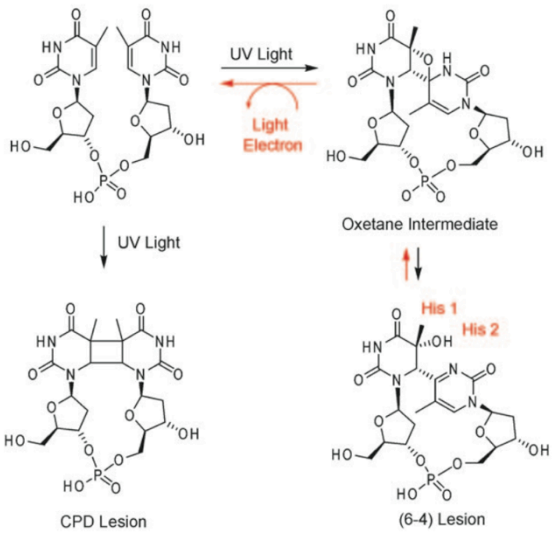

Fig. 22: Reaction illustrating the two well-known UV-damage photo-products: CPD and (6-4) Lesion.

The enzymes involved in repairing these lesions, the CPD and 6-4 photolyase, are very well-known and extensively documented including their X-ray structure and detailed mechanism of resolving the lesion. We have obtained E. coli expression plasmids from the lab of Dr Thomas Carell and one of the enzyme, the E. coli CPD PL, has already been expressed and purified to homogeneity as shown in the Figure 23.

1 2 3 4 5

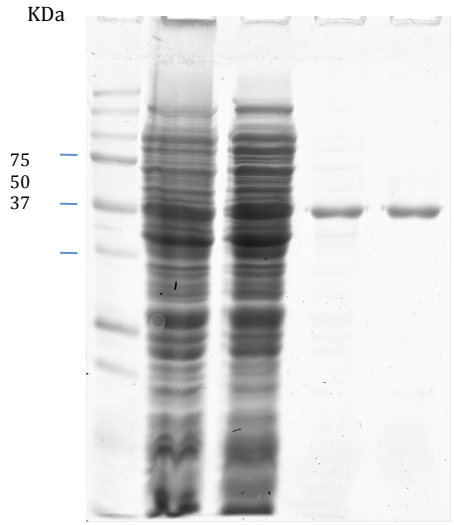

Fig. 23: *Purification of E.coli CPD photolyase. Profiles of proteins fractionated at each purification step. The enzyme (50kDa) elutes from the Strep-Tag column in two fractions. Electrophoresis was performed using a 12.5% SDS polyacrylamide gel, and the gel was stained with Coumassie Brilliant Blue R-250. Lane 1, Marker; lane 2, before strep-Tag column (Input); lane 3, run-through, protein bound to the Strep-Tag column; lane 4, flow-through fraction from the Strep-Tag column (fraction1); lane 5, flow-through fraction from the Strep-Tag column (fraction 2).*

The expression and purification of the (6-4) PL are on-going and initial data are promising. The enzymatic activity of both enzymes will be established through standard protocols that are well defined in the literature.
The enzymes will be used following L-ChIP to repair DNA lesions generated by UV irradiation. The introduction of this repairing step preceding PCR amplification will most likely alleviate the low yields observed in LChIP-seq experiments. Once DNA damages reduction has been assessed also ChIP'ed DNA recovery was improved. The establishment of the best condition for L-ChIP method now allow understanding the dynamics involved in the global DNA-proteins interactions.
Because chromathin immunoprecipitation (ChIP) assay was the main technique employed in ATLAS project to assess the UV-Laser mediated crosslinking between DNA and proteins, many tests were done to increase the efficiency and selectivity of LChIP method.
A universally applicable linear DNA amplification technology (LinDA) has been developed and validated for ultra-small amounts of DNA and for ChIP-seq and reChIP-seq studies with extremely small cell numbers. Then LinDA was modified in several aspects:

- Adaptation of LinDA to use with tissue sections (PAT-ChIP-LinDA-seq),

- Modification of the procedure such that LinDA generates DNA that can be directly used for Illumina-based sequencing and allows global studies with entirely PCR-free ChIP-LinDA-seq technology,
- Modification of the technology such that it is compatible with high-throughput automatic liquid handling.

Together with the application for the study of chromatin architecture Partner 11 thus developed a repertoire of technological applications that can be integrated in high throughput personalized medicine analyses.

A central question is how a single molecule, like the all-trans retinoic acid (ATRA), can set-up the sequence of temporally controlled events, which finally lead to the cell-physiological changes that characterize a differentiated cell. Previous studies provided for the first time a Systems Biology view of the ATRA-induced signalling pathway diversification through different regulatory decisions characterized at different time-points during differentiation. The comprehensive view of the retinoic acid (RA)-induced signal transduction events inferred from this study is still limited: only about 30% of the NR binding sites can be associated with the regulation of nearby genes, thus limiting the power of a systematic analysis of NR binding. These ~70% intergenic binding sites likely comprise regulatory elements that establish contacts with promoters and/or regulatory elements through 3-dimensional chromatin architecture, such as looping. Taken this point in consideration, temporal 3D chromatin organization at high resolution by following recently described methodologies like ChIA-PET or HiC/TCC has been reconstructed. Both approaches combine proximity-based ligation with massive parallel sequencing to assess long distal chromatin interactions but diverge slightly in their technical concept. Both ChIA-PET and HiC/TCC have an important drawback. A huge amount of cells is required for each assay (at least 25 million cells for HiC and more than 70 million cells for ChIA-PET assays), which becomes a limiting factor when assessing the chromatin architecture in large experimental series or biological compartments comprising limited cell numbers (stem cells, cancer-initiating cells, cell compartments in early development, etc.). Furthermore, both procedures involve PCR-based DNA amplification prior to massive parallel sequencing which implies a significant risk of sequence bias. To overcome these limitations, ChIA-PET technology, in which PCR amplification steps are replaced by LinDA, a single-tube linear DNA amplification method recently developed in Partner 11 laboratory and partner RU has been implemented. The ChIA-PET-LinDA-seq implementation is currently applied to the F9 differentiation model, specifically for reconstructing in a temporal manner the three-dimensional chromatin interactomes for key components like RXRa or RNA polymerase II (Figure 24). ChIP-seq data sets, like those generated for the RXR/RAR or Glucocorticoid and Estrogen nuclear receptors and CTCF or histone modification markers, will then be integrated in the interactome information to infer spatial organization in the context of newly characterized long distance interactions.

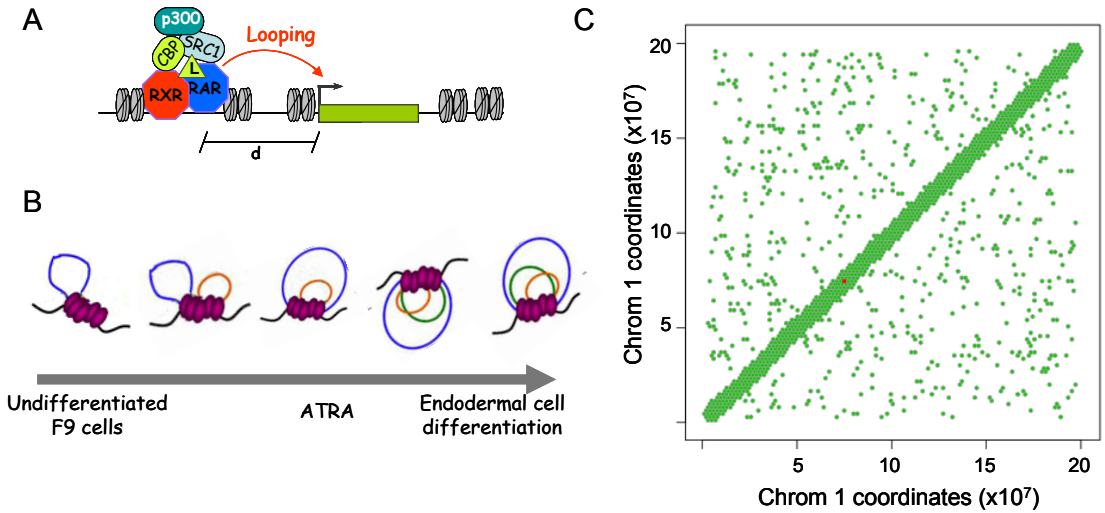

Fig.24: ChIA-PET Proximity-based ligation method applied for characterizing the 4D chromatin organization associated to the RA-induced F9 cell differentiation. *(A) Schematic representation of the intergenic binding sites, which get into contact with promoters/regulatory elements by the means of chromosomal architecture. (B) Illustration of the RA-induced F9 cell differentiation in the context of the temporal three-dimensional chromatin organization (4D). (C) RXRa Inter-chromosomal interactions (chromosome 1) characterized by applying ChIA-PET methodology. The illustrated example has been assessed in a 6 hours ATRA treated sample.*

L-ChIP efficiency has been determined by comparing with conventional formaldehyde-mediated crosslinking and assessing well-known promoter regions. In the first period several Laser settings were tested in order to find the best one, resulted to be 2Khz 7uJ at 260nm. So, RU and SUNAP performed these assays optimizing the conditions for efficient UV-crosslinking (2Khz 7uJ for 1 minute of irradiation time) followed by ChIP-qPCR. Initially, ChIP assays were done following the standard protocols with low number of starting cells. These experiments showed that the recovery after PCR was low as compared with yields obtained with conventional chemical crosslinking. This was likely due to impairment of DNA amplification due to pyrimidine dimers formation (see Figures 21-23). Hence, the DNA damage was been evaluated as the likely reason of low ChIP yields. Indeed, after the UV-laser treatment, pyrimidine dimers are formed which strongly impaired the DNA amplification. This let us to improve the laser ChIP protocol by introducing CsCl gradient and then Urea. The goal is to gain insight into the mode of interaction of proteins associated with chromatin. In the classical formaldehyde cross-linking approach, protein-protein as well as protein-DNA interaction are covalently crosslinked. In Laser crosslinking, however, the expectation is that only protein-DNA interactions can be fixed. The

principles behind the cross-linking of proteins to DNA are currently unknown and the experiments performed aim to determine which factors can be crosslinked and to establish the principles. It is for example expected that stacking of phenylalanine between a pyrimidine pair could be efficiently cross-linked (both the phenylalanine as well as the pyrimidines can be excited at 260nm). Classically, pure chromatin can be obtained using CsCl density gradients following sarkosyl lysis of the cells and extensive washing of the chromatin. Pilot experiments showed that free proteins could be readily removed from chemical crosslinked chromatin but less efficient from laser crosslinked chromatin. Therefore, RU and SUNAP established a novel protocol by introducing Urea as detergent at 4M. Urea was used with the intention to better denature, dissolve/solubilize free proteins and hence to more efficiently and instantaneously inhibit enzymatic degradation of nucleic acids during isolation. Chromatin purification was finally done by CsCl isopycnic centrifugation. This yielded pure chromatin for chemical as well as laser crosslinked material. The use of a CsCl gradient for chromatin purification allows purification of chromatin from the contamination of non-chromatin proteins, lipids, and of non-cross-linked DNA that may be present in the sample. Purified cross-linked chromatin was subsequently used to perform ChIP and LChIP using antibody towards H3K4me3 and Western blot to detect H4 histone and H3K4me3 histone modification (data not shown). First characterization of proteins covalently linked to DNA was performed by Western Blot analysis of chromatin fractions collected from CsCl density centrifugation from chemical as well as laser crosslinked chromatin. Antibodies against proteins that directly bind to DNA, such as histones, as well as proteins that are thought/known to be recruited to chromatin via protein-protein interactions such as the HDAC2 and other proteins protein were used (figure 25 below).

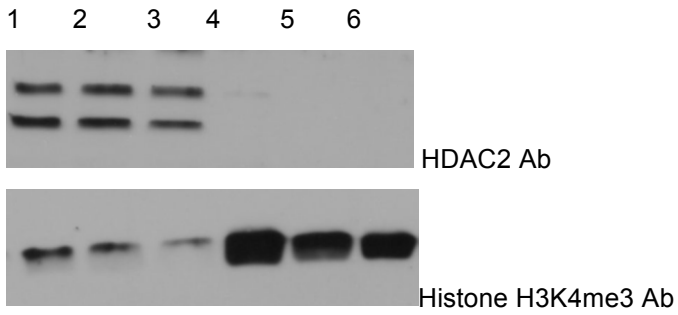

***Fig. 25**. Western blot detection of H3K4me3 (Diagenode), dilution 1:1000 (top figure) and HDAC2 (Biomol), dilution 1:1000 (lower figure) derived from: formaldehyde cross-linking chromatin samples 1, 2, 3 and laser cross-linking chromatin samples 4,5, 6*

As the laser is supposedly able only to crosslink protein to DNA and not protein-protein, the expectation is that the histones and other transcription factors are very efficiently cross-linked whereas factor that depend on protein-protein interaction are absent or very negligible. In Western Blot, the signal was compared between H3K4me3, a direct interactor of DNA, and HDAC2 that is recruited to DNA via protein-protein interactions. The analysis revealed that histones were indeed crosslinked by chemical as well as laser whereas others such as HDAC2 was only detected in chemical crosslinking. Note that the relative intensity of the histone H3K4me3 signal is much higher in Laser crosslinked than in chemical crosslinked chromatin. The reverse is observed for the presumed indirect interacting HDAC2. This strongly suggests that laser induces protein-DNA, but not protein-protein crosslinkings. To gain a comprehensive analysis of proteins

that can or not be crosslinked to DNA with Laser, a global proteomic analysis using laser and formaldehyde crosslinked chromatin has been started. Partner RU has acquired a state-of-the-art Mass Spectrometer (Q-exactive) and is performing the analysis. This analysis will provide insight into the proteins that can be crosslinked and presumably are direct DNA-binding factors and about the principles and requirements of the mode of interaction that permits/facilitates the crosslinking reaction. To assess the quality of the LChIP and ChIP experiments, LChIP-qPCR versus chemical ChIP-qPCR comparison was performed. The observed low efficiency of PCR-mediated amplification of laser cross-linked DNA was likely due to DNA damage (pyrimidine dimer formation, as explained above) and prevented a meaningful direct comparison of LChip-seq with chemical ChIP-seq. Differences in ChIP recoveries were reduced when a genomic region with a low content in A-T (and so G-C rich) bases was used in PCR amplification. L-ChIP'ed DNA required more cycles of amplification than formaldehyde cross-linked sample, as reported in the end-point PCR at 25 and 35 cycles (Figure 26).

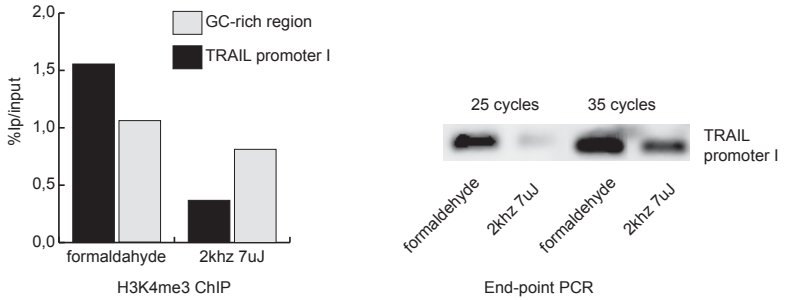

Fig. 26 *Comparison between L-ChIP-qPCR versus chemical ChIP-qPCR.*

Given the difficulties in reliably measure DNA in input and after ChIP in the case of Laser irradiated cells, we assessed the degree of crosslinking by performing Western Blot analysis. An example is provided in Figure 27. Immunoprecipitation experiments were performed on pure chemical and laser cross-linked chromatin using antibodies against CTCF, a transcriptional regulator protein known to bind directly to DNA and other proteins followed by Western Blot. Figure 27 clearly shows that CTCF is efficiently and comparably cross-linked following laser (L) and chemical (C) cross-linked chromatin providing further evidence for the suitability of the laser crosslinking method.

IP Input

L C L C

***Fig. 27**: CTCF efficiency and comparison to crosslink induction after laser (L) treatment and chemical (C) cross-linked chromatin*

Next, the L-ChIP sample from 350X10^6 MDA-231ERα-eGFP cells, laser cross-linked at 2KHz 7uJ 260nm, purified by CsCl gradient and co-precipitated with H3K4me3 antibody (Diagenode), was processed for analysis on the illumina GAIIx for high throughput sequencing (Figure 28). The UCSC genome browser screenshot shows a comparison between ChIP-seq H3K4me3 HCT sample (upper track) and LChIP-seq H3K4me3 MDA cells (lower track). Although the yield DNA derived from LChIP H3K4H3 experiment is lower than chemical ChIP, screenshots reveal that the LChIP-seq experiment worked perfectly with peaks at the transcriptional start sites. Even though the tracks are from different cell types, we observe complete overlap in these particular genomic regions. This result provides first proof-of-principle that the LChIP-seq experiment works. It is clear that the LChIP method need to be optimized to obtain higher yields so that lower amount of input chromatin can be used. The bottleneck is the DNA damage that impairs PCR amplification and sequencing.

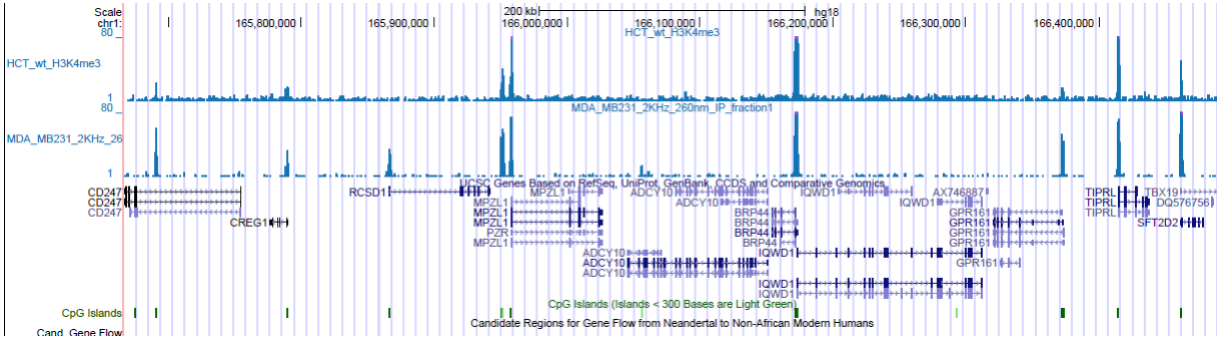

***Fig. 28:** UCSC sreen shot. Comparison between ChIP-seq H3K4me3 HCT sample and L-ChIP-seq H3K4me3 MDA cells*

Once DNA damages reduction has been assessed (by reducing the total amount of energy hitting the samples) also ChIP'ed DNA recovery was good enough as shown in Figure 29 below.

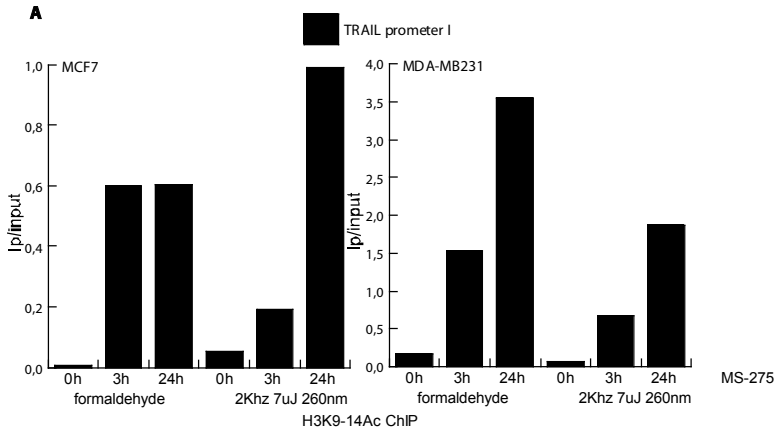

Fig. 29: *ChIP recovery on selected promoter genes after immunoprecipitation against H3K9-K14Ac*

A well-studied TRAIL promoter region was used to establish generally applicable LChIP protocols. Tumor Necrosis Factor-related apoptosis inducing ligand (TRAIL), a member of the TNF superfamily of death inducing ligands, has been identified as a powerful activator of programmed cell death in tumour cells while sparing normal cells. Previous observations revealed that TRAIL expression is up-regulated in cells treated with histone deacetylases inhibitors (HDACis), in particular MS-275 (or Entinostat). TRAIL up-regulation is triggered by the increase of the acetylation level of histone H3 (H3K9,14Ac) and of the trimethylation level on lysine 4 of histone H3 (H3K4me3) on its prometer region. In order to study the dinamics regulating TRAIL expression we used LChIP to investigate the levels of acetylated and trimetylated histone H3, using as control conventional ChIP. As shown in Figure 29 the TRAIL promoter region I is hyperacetylated in breast cancer cells, MCF7 and MDA-MB231 (but also in haematological cancer cells, such as U937 and NB4-data not shown), treated with MS-275 5μM upon 3 and 24 hours of treatment in a time-dependent manner. Higher levels of promoter-associated histone H3 acetylation were observed in all MS-275-treated cells, compared with the untreated parental cells. In Figure 29 H3K9,14Ac ChIP in MCF7 (left) and MDA-MB231 (right) cells are shown for only illustrative purposes. In summary, MS-275 treatment induced hyperacetylation and hypermethylation of histone H3 in all tested cell lines and this regulation is time-dependent. Although the changes in H3K4me3 were observed, the basal levels were much higher than those for H3K9,14Ac. The increase in H3K9,14Ac was found to be the most pronounced, where basal acetylation levels were the lowest. Global histone acetylation was increased in every cell line tested. Studies of dynamic activation of RARß promoter upon 24 hours of ATRA 1μM treatment were thus performed in NB4 cells and MDA-MB231/RARa -eGFP, as shown in Figure 30.

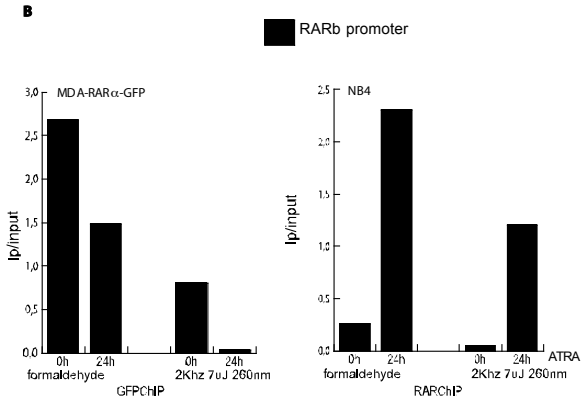

Fig. 30: *ChIP results on transfected cells and NB4 wild type ones. The data are referred to recovery on RARb promoter region with and without ATRA treatment.*

The enrichment of RARα protein on RARß promoter was revealed by direct immunoprecipitation against RARα protein (in NB4 cells) and also by indirect immunoprecipitation against the eGFP protein (in MDA-MB231/RARα -eGFP). Higher level of promoter-associated RARα was observed in ATRA-treated NB4 cells. Instead, in MDA-MB231/RARα -eGFP the RARα presence on the RARß promoter seemed to be reduced upon ATRA treatment. DNA purified after immunoprecipitation with anti- RAR and GFP antibodies was evaluated by PCR using primers targeting the RARß promoter region. In Figure 30 are shown the eGFPChIP in MDA-MB231/RARα-eGFP (left) and RARα-ChIP in NB4 (right) cells. Comparing the conventional RARα ChIP to the L-ChIP, the recoveries showed a similar trend, revealing a good occupancy of RARα on RARß promoter and a high fold variation of recovery after the treatment of NB4 cells with ATRA. Notably, the different cell systems used (NB4 and MDA-MB231/RARα-eGFP) suggest differences in the RARα-dependent pathways upon ATRA treatment. Of course the presence of PML-RARα in NB4 cells may account for those differences. Indeed, the ATRA effects in MDA-MB231/RARα-eGFP will require further investigations. Data arising from these ChIP experiments let improve the protocol for LChIP and to apply it coupled with sequencing on the whole human genome (L-ChIPseq). After the establishment of crosslink, the overcoming of DNA damages induction and the improvement of ChIP protocol, the geometry of irradiation was also studied. In particular a microfluidic device coupled with the Laser source was utilized to induce the crosslink (against the cuvette mode). Following, in Figure 31 some experiments summarizing the procedure have been illustrated.

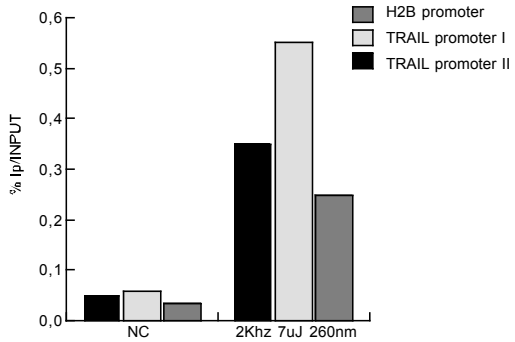

Fig. 31: *ChIP experiment. Irradiation condition= 2kHz 7μJ 260nm; speed= 25μl/minute*

So, in a selected condition (2kHz 7μJ for 8 times) and with a speed equal to 25μl/minute, ChIP experiment was done. Data shown in Figure 31 were referred to a ChIP experiment against 3meK4H3, in which different genomic promoter regions are analysed in response to crosslink induction. UNINA2 partner sets up and applies LChIP to the analysis of selected tissue cellular populations. This system will use frozen tissue slides via the connection with a refrigerated allocation and will allow for the first time to identify and crosslink selected populations that could be than captured. Moreover DNA damage occurring during the set-up of LChIP will be assessed. Sections of thickness of 8-20 μm have been prepared by using microtome and kept frozen. Tissue sections this way prepared and allocated on a cooling devise, have been irradiated at 2kHz, 8 mJ at 260 nm. At first we were able to confirm the results for the whole tissue. However, we also examined microdissected cells in parallel. To this aim the UV laser was set-up to separate a group of target cells from the surrounding tissue. We could confirm the irradiation via the generation of thymidine dimers to an extent similar to the experiments carried out in living cells (Figure 32). Contemporary, we could confirm that at the chosen parameters of irradiation the amount of DNA damage (evaluated via H2AX expression levels) was compatible to the one obtained from the irradiation at these settings in living cells (both in the microfluidic device or in the cuvette). When the ChIP protocol was applied we could confirm the method in whole tissue whereas the amount of microdissected cells did not allow the application of the method (Figure 32). Likely, the optimization of protocols allowing the use of minimal amount of cells will allow also the use of microdissected cells. The test of LChIP to the analysis of selected tissue cellular populations indicates the feasibility of the method. Further attempts to optimise the conditions for the use of minimal amounts of cells are needed to better define the method.

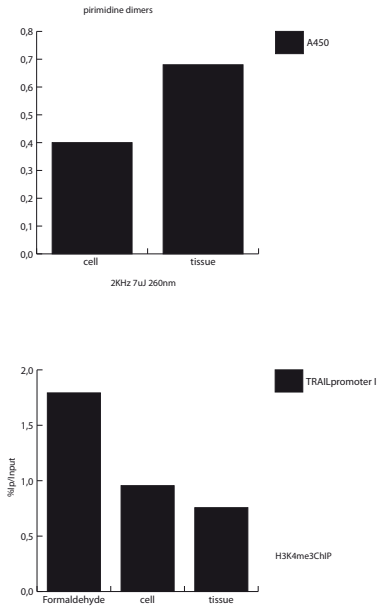

Fig. 32: *Dimers evaluation and ChIP assay on deriving from tissue cells.*

The ATLAS consortium as a whole has worked to optimize ChIP assays on low cells numbers as well as on developing methods of amplification.
Diagenode has focused on optimizing protocols for the amplification of ChiP'ed DNA isolated from low number of cells. (e.g. using 10000; 1000 cells per LChIP). Although a few publications have shown the feasibility of ChIP assays starting from 10000 cells, they also showed some discrepancies and limitations in terms of the amount of DNA recovered, as well as the lack of sufficient genome coverage after whole genome sequencing. Having a strong expertise in ChIP protocol setup, we have proceeded step by step by also improving the ChIP assay itself on reduced number of cells. All steps have been thoroughly optimized. Are listed below some critical parameters:

-Percentage of formaldehyde: 1% FA remains the standard

-Cell counting with an automated cell counter to reduce ChIP result variability

-Use of the DiaMag proteinA-coated magnetic beads

-Antibody titration

-Chromatin/antibody incubation for 16h. Addition of beads for 2 hours only to minimize aspecific binding to the beads

-Reduction of sample handling (one step cell lysis, one step phenol/chloroform extraction, reduction of sample pipetting/handling throughout the experiment)

-Use of low retention tubes to reduce sample loss

-Use of stringent was buffers to decrease background

-Use of 2 different carriers for DNA precipitation in ethanol after immunoprecipitation to increase DNA recovery

ChIP on 10000 cells for different histone marks have been successfully performed as revealed by Figure 33.

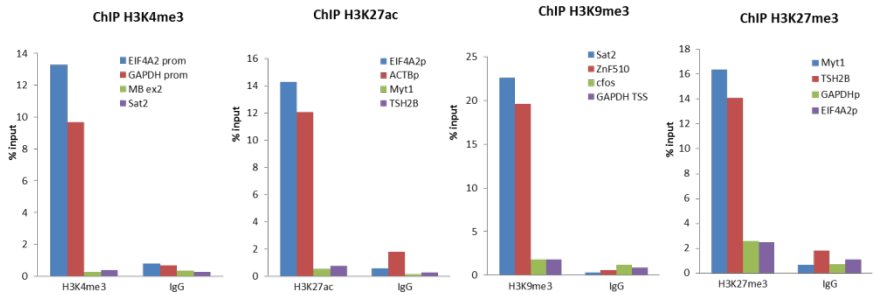

***Fig. 33*: ChIP efficiency on 10000 cells.** *ChIP assays were performed on 10000 Hela cells with Diagenode H3K4me3 (0.25 µg/reaction), H3K27ac (0.1 ug/reaction), H3K9me3 (0.5 ug/reaction) and H3K27me3 antibodies (0.25 µg/reaction). Corresponding amount of IgG was used as control. The qPCR was performed with primers for corresponding positive and negative loci.*

The amount of DNA recovered after ChIP is very limited and varies, depending on the antibody used for the immunoprecipitation. For some histone marks, like H3K4me3, we recovered grossly 1ng of IP'd DNA (at a concentration of 15 to 30 pg/µl) per ChIP reaction on 10 000 cells. For other marks more widely spread along the genome (such as H3K27me3), a few nanogram of DNA were recovered after ChIP. During the course of the project, partner CERBM-GIE and partner

RU have successfully developed methods of amplification from suboptimal amount of DNA. These methods are based on linear amplification with the T7 DNA polymerase, and, although very efficient, are quite fastidious and not a really compatible with a kit format. Diagenode has thus explored the compatibility of amplification of low amount of ChIP'ed DNA with the PCR-based technology that works by converting randomly fragmented DNA into a library of inherently amplifiable DNA fragments of defined size. The advantages of that method are numerous:

- All steps are performed in a single tube limiting risks of contamination

- The technology is suitable for amplification of picograms amount of DNA

- The protocol allows combined amplification and library preparation leading to a sequencing-ready preparation for the Illumina plateform on a multiplexing format

-It works well on slightly degraded DNA

To test the amplification and library preparation using that technology, a single ChIP reaction was performed using H3K4me3 antibody on 10000 cells. 17 pg of immunoprecipitated DNA were used to start the library preparation. As control, a ChIP assay using the same protocol was performed on 100000 cells. Library preparation on DNA immunoprecipitated from 100000 cells was done with 35 pg of DNA. The samples were multiplexed and then sequenced on an Illumina GAIIx analyzer.

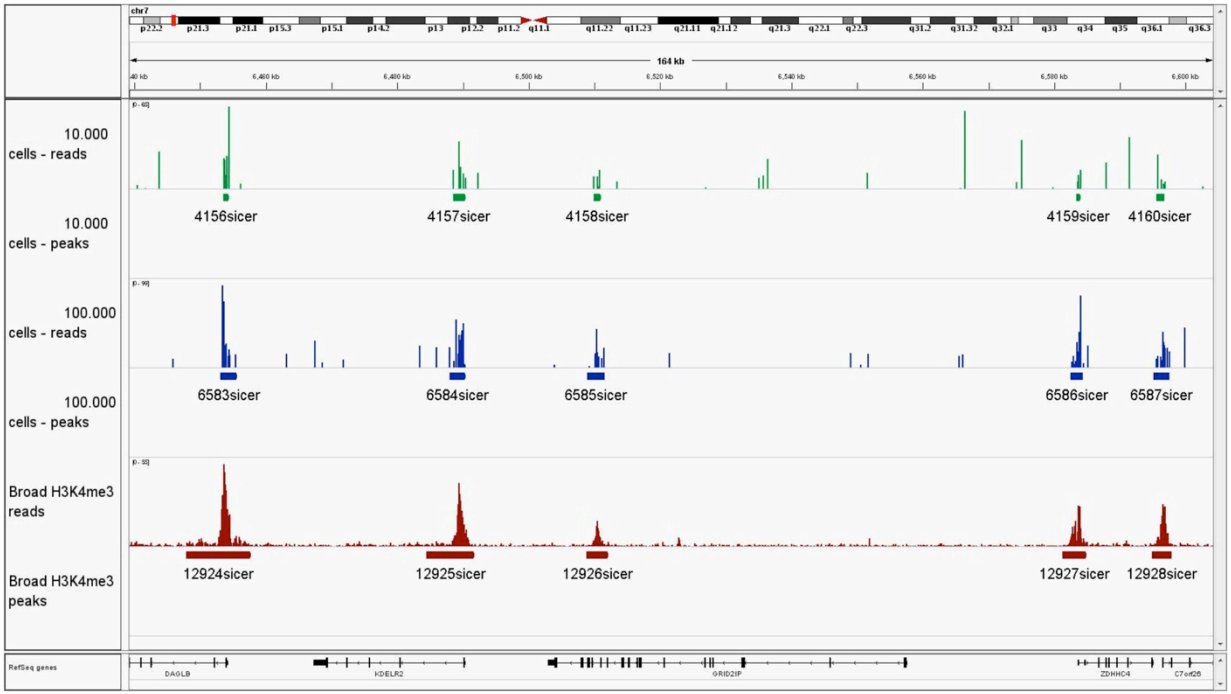

Fig. 34: *ChIP was performed on sheared chromatin from 10000 or 100000 Hela cells using the ChIP protocol we optimized and the Diagenode H3K4me3 antibody. The IP'd DNA was amplified and transformed into a sequencing-ready preparation for the Illumina plateform.. The amplified DNA was subsequently analysed on an Illumina® Genome Analyzer. Cluster generation and sequencing were performed according to the manufacturer's instructions. The 36 bp tags were aligned to the human genome using the ELAND algorithm.*

To analyze the accuracy of the data we generated, sequencing data were filtered using the peak calling SICER software to find the enriched regions in the alignment (Table 5) and then crosscompared (10000 cells versus control, 10000 cells versus Encode data). Comparison of the peaks obtained from 10000 cells to those obtained from 100000 cells revealed that most of the 10000 cells peaks are confirmed by the data set generated on 100000 cells. Most importantly, 90% of the peaks obtained from 10000 cells correlate with the ones identified by the Encode data used as a standard reference. This percentage raise up to

98% in the Top40 peaks detected. All together these data prove the peaks identified with 10000 cells are “real peaks”. The combination of our ChIP protocol on 10000 cells with amplification by produce reliable results with few background.

	10 000 cells	**100 000 cells**
Unique reads	331244	732700
Duplicate ratio	94,25	95,19%
Read in peaks %	18%	56,42%
Total peaks	8745	12515
Promoter peaks	68,5%	78,58%
Coding peaks	55,6%	61,28%
Gene rich peaks	98,5%	99,35%
Overlap with 100 000 %	87,1%	100%
Broad total peaks	26183	26183
Overlap with broad %	90,62%	94,87%
Total top40 peaks	3498	5006
Broad total top40 peaks	10479	10479
Top40 overlap with broad %	97,89%	99,46%

Table 5: *Sequencing data obtained with our ChIP protocol in combination with the ThruPLEX kit on 10000 and 100000 cells were analyzed with the peak caller SICER. These data were compared with those generated by the Broad.*

Now that the LChIP technology is fully mature, the last step will be to interface it with the protocol developed by Diagenode. Diagenode’s protocol has proven to be very robust and will be launched under a commercial kit under the name the Diagenode True MicroChIP kit during the course of October 2012. That kit will be the first of its kind to be launched on the market. Thanks to the ATLAS consortium, the epigenetic community will then now have access to new tools, from efficient chromatin crosslinking, to optimize ChIP assays for low amount of material, to various methods of amplification PCR or non-PCR based. The amplification module, marketed as the Diagenode True Amplification kit, will be launched either as a stand-alone product or combined to the True MicroChIP kit, allowing the customers the flexibility to choose their method of amplification depending on their needs.

The potential impact and the main dissemination activities and exploitation of results.

ATLAS is a multidisciplinary research platform with the aim of developing a fully new technological approach to allow the global screening of DNA bound proteins and chromatin modifications using dynamic and time ranges currently unreachable. This consortium integrated a wide variety of competences to develop and apply a new technical approach to understand and to model biological processes at different levels of organization (genome, transcriptome, proteome, phosphoproteome, interactome, regulatory networks, physiological processes). Actually no tools are present which reach these targets in a dynamic manner and so ATLAS works to answer to this specific requirement.

ATLAS integrated dispersed capabilities of partners from 8 European countries and assembled the critical mass required to enable new global approaches, by networking the necessary expertise to secure European excellence and competitiveness, and to explore new directions in the research field.

Consortium planned to deliver new knowledge on basic biological processes relevant to health and disease. The quantitative data delivered served as the basis to design robust models using computational biology approaches.

The overall objective of ATLAS was to establish a novel global ChIP technology based on highly efficient, precise, robust and reproducible laser-assisted DNA-protein crosslinking (termed “L-ChIP” and “L-ChIP-chip”). Development of this innovative technology overcame the limitations imposed by the conventional formaldehyde-based chemical crosslinking and allowed the deconvolution of genomic information into transcription factor and epigenetic mediator-modulated executor networks with unprecedented accuracy, sensitivity and precision at a dynamic range which is several times larger than that possible when using conventional ChIP methodology. The technique was established to allow genome-wide studies of human genome.

In addition, the ATLAS consortium developed this technology further to make it compatible with fluorescence-activated cell sorting. Thus, individual cells with pre-defined “marker” characteristics, such as cells of a particular differentiation status, for example of the hematopoietic lineage, leukemic blasts, or cells that have characteristics of cancer stem cells, can be selectively laser-crosslinked and their epigenome and genome-encoded information analyzed. In addition to studies done for ATLAS purpose and technique development, this characteristic will allow a multitude of studies, including mechanisms of transcription regulation by factor-DNA recognition (stochastic vs. productive DNA interaction within time frames covering second to minute scales), as well as genetic and epigenetic aberrations of gene expression in cancer (stem) cells, cell lineage analysis, and studies to distinguish gene regulation originating from direct and indirect binding to “response elements”, respectively.

In close collaboration with one of the SME partners, a specialist in laser production, the ATLAS consortium developed both “open” and “closed” (pre-adjusted) laser prototypes for the various possible ChIP technologies and had as perspective to provide such laser systems to the scientific community, either through the industrial partner or through a newly established spin-off company. The expected high efficiency, accuracy, selectivity and the extraordinary large dynamic range of laser-ChIP and laser-ChIP-chip technology allowed to perform genome-wide deconvolution experiments, which are impossible to date.

Among the possible scientific advancements obtained during ATLAS project, following are the most important:

Selective factor-DNA crosslink allowed precision mapping of binding sites repertoires. Using ATLAS technology non-specific protein-protein crosslink will be negligible and for the first time it will be possible to study pure factor binding to DNA with unmet accuracy, thus high precision factor (or epigenetic modification) maps can be generated. Comparison with conventional chemical crosslink will facilitate to distinguish between direct and indirect (through protein-protein contacts) DNA binding. Such information is of high mechanistic value. By modulating the parameters (wavelength, delay time to first pulse, circularization) of the second pulse, we will as well explore the possibility of photocrosslinking also protein-protein complexes.

Novel strategy of experimental design – important mechanistic questions can be addressed. The ATLAS technology will potentially change the actual view of promoter function and gene regulation, leading to novel concepts of gene expression. Indeed, the comparison with data from formaldehyde crosslinking

will most likely lead to novel classification/distinction of binding sites in enhancers versus promoters and/or to a completely revised view of enhancer and promoter function. Moreover, the efficiency and specificity of this approach will allow to define cellular context specific regulation in a dynamic time frame, which is currently unthinkable due to technical limitations. The applications of this technology will most likely open a new strategy of experimental design with very wide applications.

Knowledge transfer and enforcement of other EU projects. The ATLAS technology will re-enforce the contacts among different multidisciplinary European groups and will establish a core technological center not only for ATLAS members but also for partners of several EU IP/STREP programs as indicated above. This mode of tight consortia linkage will undoubtedly strengthen the scientific competitiveness of the European partners involved.

New dimension of ChIP analyses with SORT-ChIP. The combination of FACS and ChIP will open an entirely new dimension of genome-wide analysis. At the moment, complex biological samples such as blood or bone marrow can only be analyzed as a whole. FACS-laser-ChIP will allow selective crosslinking at the single cell level and combine the potential of FACS-based cell sorting with the power of genome-wide transcription factor binding and epigenetic mapping analysis by ChIP and ChIP-chip. Moreover, features of minor but highly important cell populations (e.g. cancer stem cells) will become amenable to ChIP-chip analysis due to the selection potential of the FACS and the highly efficient crosslink by the dual pulse fs laser.

Economical impact. The development of the laser-ChIP and FACS-laser-ChIP—based technologies will have an important economical impact given the tremendous rapid expansion of the field and the use of ChIP for basic, but also applied and industrial/pharmaceutical, research. The project allowed the development of closed systems that can be marketed either by the industrial partner, or in the context of a spin-off company that can be created from the accumulated know-how.

Moreover, the project will strengthen the competitiveness of the participant LightCon company which had the opportunity to improve its expertise within the project and to profit from the transfer of know how from the collaboration with outstanding experts from different fields of life science and technology. Finally, ATLAS-developed technology increased LightCon competence and facilitated its efforts to enter in a biological area of application.

Strategy

We have entered a phase of genome function analysis by which we can map regulatory proteins and machineries as well as epigenetically relevant DNA and chromatin modifications (i.e. post-translational modifications of histones that may constitute an “epigenetic code”, presence of histone variants, nucleosome densities) at the genome wide level. To overcome the major limitations for the use of the conventional ChIP-chip technology which are nearly exclusively due to the limitations of the initial chemical crosslinking step, the ATLAS consortium has gathered an international multidisciplinary consortium of high calibre mathematicians, physicists, chemists, molecular biologists (both array specialists and signal transduction specialists) and molecular oncologists with the aim to replace this step by laser-assisted photo-crosslinking and establish a ChIP-chip technology in which the precision and reliability of the ChIP matches that of the array technology. In addition the novel laser-ChIP approach opens a large spectrum of additional experimental options that cannot be addressed with current technologies.

Step by step, the Atlas activity could be summarized as follows:

At the first level ATLAS developed a laser system that is specifically adapted to DNA-protein crosslinking. We have already provided proof-of-principle that a rather “primitive” UV laser can be used for laser-ChIP at efficiencies, which are several times higher than those of conventional formaldehyde-based crosslinking (as reported in Annex 1 document).

In the second phase this novel laser system-ChIP was set up and validated in two modes of operation in parallel. On the one hand laser-ChIP was applied to individual promoters of high scientific interest to explore novel options of the laser-ChIP technology (as explained in detail in S&T results/foregrounds section), on the other hand laser-ChIP-chip was set up and used to address genome function-related questions.
A particular strength of the ATLAS project is its tight link to three other European consortia; this collection of top specialists used laser-ChIP technologies to address very distinct aspects of genome complexity and deconvolution of genome-encoded information. This configuration is of mutual benefit: ATLAS provides them with a novel technology that enhances their experimental capacities, while these consortia provide ATLAS with very expensive materials (genomic tiling arrays) for validation of its technology.
In its third phase ATLAS developed an even more challenging technology, which allows performing genome-wide deconvolution studies in pre-defined subsets of complex biological cell populations. This technology comprises the combination of fluorescence-activated cell sorting (FACS) with the laser ChIP. The technology was developed in two steps: First ATLAS used a discontinuous mode of operation to determine key parameters, in particular the sensitivity (minimal number of cells necessary for ChIP) and selectivity (multidimensional selection of cells). The second step was technically most challenging but offers the highest scientific potential. ATLAS constructed the prototype of a FACS containing a dual pulse femtosecond laser for in situ crosslinking at the single cell level during sorting. With this FACS-laser set-up it will be for the first time possible to crosslink in a heterogeneous population of cells selectively those that are recognized by the FACS according to pre-defined parameters (e.g., cell dimensions, cell surface markers).
Potential applications of such technologies are obviously not only widespread but future development of the field will demand such an option to apply ChIP and ChIP-chip assays to “real” biological samples, which are inherently composed of multiple cell populations. In this field, some experiments were just done (as reported in results section) and resulted interesting for further investigations.

Contribution that requires a European approach

It is clear that neither of individual partners can address this complex multidisciplinary approach either on local or on national levels. Only a unique combination of biologists, chemists, physicists, clinicians, mathematicians, medical doctors and persons from biotechnology industries (SME) together with a great contribution from the European Union were able to achieve the expected impact. In the past, some of the partners established a tight collaboration and got preliminary results which could not be followed up without the creation of this consortium. Although all partners are getting some support from their National Foundations, only joined efforts along with a support from the European Union significantly influenced the quality of this research project. We are not aware of any other projects involving experimental biology, data mining, mathematical modelling, informaticians and molecular medicine applied to chemistry and physics. Moreover, the central participation of SMEs allows the development of commercial tools and implements the connection between the industrial and academic scientific work; SMEs enjoyed benefits from the research approach and its application for the creation of LChIP technology; academic partners received from the direct binding with industries for an immediate commercial view of the products of this consortium.
The participation in the consortium of partners performing different, but complementary, investigations enhanced the possibility of exploiting the novel findings of the project.
ATLAS improved Europe’s innovation performance by stimulating a better integration between research and innovation and by working towards a more innovation-friendly policy.
On the bases of our good results, one of our long-term goals is to enhance the inclination for turning research into useful and commercially valuable innovations.

We believe that successful development of this project based on tight collaboration between groups will help us in the future to develop the “European Centre of Excellence” for technological excellence.
All partners represent the leading European groups in their field of research and had all potential to achieve the main goal of this very ambitious project. Only the synergy of all partners (which include many disfavoured European countries and country regions) helped us to reach the defined goal but without the financial support the achievements of all impacts (listed at now) would not have been possible.

Use and dissemination of foreground

The ATLAS consortium web site is available at http://www.atlas-eu.com.

Tha ATLAS Project Logo has been designed on purpose for the consortium and is the following:

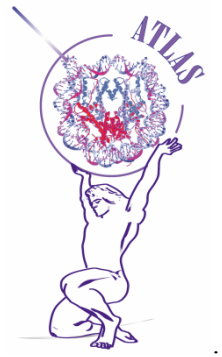

In addition to Section A and B below, diagrams and photographs illustrating and promoting the work of the project (including main videos, press releases, conferences, PhD thesis, Exhibitions, Posters, Flyers), are available on the website and have been listed in the deliverable *D36 - Final Plan for the Use and Dissemination of Foreground*, which is to be considered as an integral part of this section.

Here below is the list of main contact persons for this project:

Responsible	**E-mail**	**Beneficiary, Country**	**Beneficiary short name**
Prof. Lucia ALTUCCI, MD, PhD	lucia.altucci@unina2.it	Seconda Università degli Studi di Napoli Dipartimento di Patologia generale, Napoli, Italy	SUNAP
Dr. Arunas Varanavicius	arunas@lightcon.com	Light Conversion, Ltd, Vilnius, Lithuania	LC
Prof. Carlo ALTUCCI, PhD	altucci@na.infn.it	Department of Physical Sciences, Università degli Studi di Napoli "Federico II", Italy	UNINA
Prof. Dr. Hendrik G. STUNNENBERG	H.Stunnenberg@ncmls.ru.nl	Head of Dept of Molecular Biology, Nijmegen Center of Molecular Life Sciences, Radboud University, Nijmegen, The Netherlands	RU
Dr. Didier ALLAER	didier.allaer@diagenode.com	Avenue de l'hôpital, 1 Bat 34, GIGA Sart Tilman 4000 Liège, Belgium	DIAGENODE
Dr Jonas JARVIUS	Jonas.Jarvius@sigolis.com	Sigolis AB, Uppsala, Sweden	SIGOLIS AB
Dr. Valer TOSA	tosa@itim-cj.ro	Laboratory for Molecular and Biomolecular Physics, INCDTIM Cluj-Napoca, Romania	INCDTIM
Prof. Angel R. De LERA	qolera@uvigo.es	Departamento de Química Orgánica, Universidade de Vigo, Spain	UVIGO
Dr. Larisa PETCU	Larisa.Petcu@brinel.ro	BRINEL, Cluj-Napoca, Romania	BRINEL
Prof. Hinrich GRONEMEYER, PhD	hg@igbmc.fr	Department of Cell Biology and Signal Transduction, CERBM-GIE (IGBMC), Illkirch, France	CERBM-GIE

Section A (public)

TEMPLATE A: LIST OF SCIENTIFIC (PEER REVIEWED) PUBLICATIONS, STARTING WITH THE MOST IMPORTANT ONE

NO.	Title	Main author	Title of the periodical or the series	Number, date or frequency	Publisher	Place of publication	Year of publication	Relevant pages	Permanent identifiers[1] (if available)	Is/Will open access[2] provided to this publication?
1	Nonlinear protein – nucleic acid crosslinking induced by femtosecond UV laser pulses in living cells	C. Altucci	Laser Physics Letters	vol.9, March	WILEY-VCH Verlag GmbH & Co. KGaA	UK	2012	234-239		
2	Low-lying excited-states- of 5-benzyluracil	M. Micciarelli	Journal of Physical Chemistry A	2012, 10			2012			
3	UV laser induced		Chemical	2012, 10			2012			

[1] A permanent identifier should be a persistent link to the published version full text if open access or abstract if article is pay per view) or to the final manuscript accepted for publication (link to article in repository).

[2] Open Access is defined as free of charge access for anyone via the internet. Please answer "yes" if the open access to the publication is already established and also if the embargo period for open access is not yet over but you intend to establish open access afterwards.

	crosslinking in peptides		Communications							
4	Linear amplification for deep sequencing	W.A. Hoeijmakers	Nature Protocols	23;6(7):1026-36 Jun	Nature Publishing Group		2011		http://www.nature.com/nprot/journal/v6/n7/full/nprot.2011.345.html	
5	Single-tube linear DNA amplification for genome-wide studies using a few thousand cells	Pattabhiraman	Nature protocols	7(2)	Nature Publishing group	UK	2012	328-38		
6	The transcriptional and epigenomic foundations of ground state pluripotency	H. Marks	Cell	27;149(3) Apr	Cell press		2012	590-604	http://www.cell.com/abstract/S0092-8674%2812%2900409-6	
7	Single isolated attosecond pulse from multicycle lasers	C. Altucci	Opt Lett.	Dec,15;33(24):2			2008	943-5.		
8	Generation and application of high energy, 30 fs pulses at 527 nm by hollow-fiber compression technique	C. Altucci	European Physical Journal – Special Topics	Vol.175	EDP Sciences – Springer Verlag		2009	11-14		
9	Fiber-optic glucose biosensor based on glucose oxidase immobilised in a silica gel matrix	D.G. Mita	J Sol-Gel Sci Technol	50:437–448			2009	440-447		
10	Generating single attosecond pulses using multi-cycle lasers in a polarization gate	V. Tosa	Optics Express	Vol.17,	Optical Society of America	USA	2009	17700-17710		

11	One- and two-photon time-resolved fluorescence of visible and near-infrared dyes in scattering media	R.Esposito	Proceedings SPIE Advanced Biomedical and Clinical Diagnostic Systems VII	vol.7169 art. 7169J			2009			
12	Phase-matched generation of water-window x rays	V. Tosa	Physical Review A	Vol. 80, Art. Nr. 045801	American Physical Society	USA	2009	3	http://dx.doi.org/10.1103/PhysRevA.80.045801	
13	Extension of high harmonic spectroscopy in molecules by a 1300 nm laser field	R. Torres	Optics Express	Vol. 18,	Optical Society of America	USA	2010	3174-3180		
14	Revealing molecular structure and dynamics through high-order harmonic generation driven by mid-IR fields	R. Torres	Physical Review A	Vol. 81, art. N. (R)051802	American Physical Society	USA	2010	1-4		
15	Ultra-fast dynamic imaging: an overview of current techniques, their capabilities and future prospects	J.P. Marangos	Journal of Modern Optics	VJune 16, vol. 57	Taylor&Francis LTD	UK	2010	Invited review article: 916-952		
16	Ultra-fast dynamic imaging of matter: INTRODUCTION	C. Altucci	Journal of Modern Optics	VJune 16, vol. 57,	Taylor&Francis LTD	UK	2010	915		
17	Interplay between group-delay-dispersion-induced polarization gating and ionization to generate	C. Altucci	Optics Letters	Vol. 35,	Optical Society of America	USA	2010	2798-2800		

	isolated attosecond pulses from multi-cycle lasers									
18	Measurement of the two-photon absorption cross-section of liquid argon with a time projection chamber	B. Rossi	New Journal of Physics	Vol. 12, art. N. 113024	Institute of Physics	UK	2010	1-15		
19	High harmonic generation spectroscopy of hydrocarbons	R. Velotta	Applied Physics Letters		American Institute of Physics	USA	2010			
20	Glucose sensing based on the intrinsic time-resolved visible fluorescence of sol-gel immobilized glucose oxidase	R. Esposito	Journal of Molecular Catalysis B		Elsevier		2010			
21	Isolated attosecond pulse generation by two-mid-IR laser fields	R. Velotta	Journal of Selected Topics in Quantum Electronics IEEE		IEEE	USA	2010			
22	Attosecond source technologies: an overview of current techniques, their capabilities, and future prospects	C. Altucci	Journal of Modern Optics		Taylor&Francis LTD	UK	2010			
23	FT-IR microscopy characterization of sol–	D.G. Mita	J Sol-Gel Sci Technol				2010			

	gel layers prior and after glucose oxidase immobilization for biosensing applications									
24	Single attosecond light pulses from multi-cycle laser sources	C. Altucci	Journal of Modern Optics	Volume 58, Issue 18,			2011	1585-1610		
25	Glucose sensing by Time-Resolved Fluorescence of Sol-Gel Immobilized Glucose Oxidase	R. Esposito	Sensors	vol.11			2011	3483-3497		
26	Light assisted antibody immobilization for bio-sensing	B.Della Ventura	Biomedical Optics Express	vol.2			2011	3223-3231		
27	Gating of high-order harmonics generated by incommensurate two-color mid-IR laser pulses	M. Negro	Laser Physics Letters	vol.8			2011	875-879		
28	Isolated Attosecond Pulse Generation by Two-Mid-IR Laser Fields	V. Tosa	IEEE Journal of Selected Topics in Quantum Electronics	vol.18			2011	239-247		
29	Measurement of the two-photon absorption cross-section of liquid argon with a time projection chamber	I. Badhrees	New Journal of Physics	vol.12 art.113024			2010			
30	High harmonic generation spectroscopy	C. Vozzi	Applied Physics Letters	vol.97 art. 241103			2010			

	of hydrocarbons									
31	Single-tube linear DNA amplification (LinDA) for robust ChIP-seq	Pattabhiraman	Nature Methods	8(7)	Nature Publishing group	UK	2011	565–567	http://www.nature.com/nmeth/journal/v8/n7/full/nmeth.1626.html	
32	Phase-matching effects in the generation of high-energy photons by mid-infrared few-cycle laser pulses	V. Tosa	New Journal of Physics	Vol. 13 Art nr. 073003	IOP Publishing Ltd and Deutsche Physikalische Gesellschaft	UK	2011	17	doi:10.1088/1367-2630/13/7/073003	
33	Analysis of simulated fluorescence intensities decays by a new maximum entropy method algorithm	R. Esposito	Journal of Fluorescence	2012, Oct 19			2012			
34	POLYPHEMUS: R package for comparative analysis of RNA polymerase II ChIP-seq profiles by non-linear normalization	M. Mendoza-Parra	Nucleic Acids Research	40(4)	Oxford Journals	UK	2012	1-11	http://www.ncbi.nlm.nih.gov/pmc/articles/PMC3287170/pdf/gkr1205.pdf	
35	H2A.Z demarcates intergenic regions of the plasmodium falciparum epigenome that are dynamically marked by H3K9ac and H3K4me3	R. Bártfai	PLoS Pathogens	16;6(12):e1001223 Dec	PLOS journals		2010		http://www.plospathogens.org/article/info%3Adoi%2F10.1371%2Fjournal.ppat.1001223	
36	Dissecting the retinoid induced differentiation of F9 embryonal stem cells by integrative genomics	M. Mendoza-Parra	Molecular Systems Biology	7	Nature Publishing group and EMBO	DE	2011	538-	http://www.ncbi.nlm.nih.gov/pmc/articles/PMC3261707/	

37	Transcriptome Analysis Using RNA-Seq	W.A. Hoeijmakers	Methods in Molecular Biology	923:221-39	Humana Press		2013			
38	Evaluation of histone deacetylases as drug targets in Huntington's disease models. Study of HDACs in brain tissues from R6/2 and CAG140 knock-in HD mouse models and human patients and in a neuronal HD cell model.	L. Quinti	PLoS Curr	2010 Sep 2;2. pii: RRN1172			2010		http://www.ncbi.nlm.nih.gov/pubmed/20877454	
39	HDACs class II-selective inhibition alters nuclear receptor-dependent differentiation	A. Nebbioso	J Mol Endocrinol	45(4) Oct	the Society for Endocrinology	USA	2010	219-28	http://www.ncbi.nlm.nih.gov/pubmed/20639404	
40	Identification of tri- and tetracyclic pyrimidinediones as sirtuin inhibitors.	D. Rotili	ChemMedChem.	5(5) May 3	WILEY-VCH Verlag GmbH & Co. KGaA, Weinheim	UK	2010	674-7	http://www.ncbi.nlm.nih.gov/pubmed/20391556	
41	Characterization of sirtuin inhibitors in nematodes expressing a muscular dystrophy protein reveals muscle cell and behavioral protection by specific sirtinol analogues.	M.Y. Pasco	J Med Chem	53(3) Feb 11	American Chemical Society	USA	2010	1407-11	http://www.ncbi.nlm.nih.gov/pubmed/20041717	
42	Study of 1,4-	L .Altucci	Med Chem.	Sep,10;52(17):5			2009	496-504		

	dihydropyridine structural scaffold: discovery of novel sirtuin activators and inhibitors									
43	Molecular analysis of the apoptotic effects of BPA in acute myeloid leukemia cells.	P. Bontempo	J Transl Med.	Jun 18;7(1):48.			2009			
44	Pyrrole-Based Hydroxamates and 2-Aminoanilides: Histone Deacetylase Inhibition and Cellular Activities.	S. Valente	ChemMedChem.	Jun 5.			2009			
45	Novel N-hydroxybenzamide-based HDAC inhibitors with branched CAP group	H.Su	Bioorg Med Chem Lett	19(22) Nov 15	Elsevier	UK, the Netherlands ,USA	2009	6284-8	http://www.ncbi.nlm.nih.gov/pubmed/19822426	
46	Study of 1,4-dihydropyridine structural scaffold: discovery of novel sirtuin activators and inhibitors.	A. Mai	J Med Chem.	52(17) Sep 10	ACS	USA	2009	5496-504	http://www.ncbi.nlm.nih.gov/pubmed/19663498	
47	Pyrrole-based hydroxamates and 2-aminoanilides: histone deacetylase inhibition and cellular activities.	S. Valente	ChemMedChem	4(9) Sep	WILEY-VCH Verlag GmbH & Co. KGaA, Weinheim	UK	2009	1411-5	http://www.ncbi.nlm.nih.gov/pubmed/19504533	

48	New anacardic acid-inspired benzamides: histone lysine acetyltransferase activators	J.A. Souto	ChemMedChem	5(9) Sep 3	WILEY-VCH Verlag GmbH & Co. KGaA, Weinheim	UK		1530-40	http://www.ncbi.nlm.nih.gov/pubmed/20683922	
49	Impact of histone deacetylase inhibitors SAHA and MS-275 on DNA repair pathways in human mesenchymal stem cells	G. Di Bernardo	J Cell Physiol	225(2) Nov	Wiley-Liss, Inc	UK	2010	537-44	http://www.ncbi.nlm.nih.gov/pubmed/20458754	
50	New anacardic acid-inspired benzamides: histone lysine acetyltransferase activators.	J.A. Souto	ChemMedChem	Sep 3;5(9)	Wiley-VCH		2010	1530-40		
51	Novel cinnamyl hydroxyamides and 2-aminoanilides as histone deacetylase inhibitors: apoptotic induction and cytodifferentiation activity	S. Valente	ChemMedChem	Apr 4, 6(4)	WILEY-VCH	UK	2011	698-712	http://www.ncbi.nlm.nih.gov/pubmed/21374822	
52	Simplification of the tetracyclic SIRT1-selective inhibitor MC2141: coumarin- and pyrimidine-based SIRT1/2 inhibitors with different selectivity profile	D. Rotili	Bioorg Med Chem	19(12) Jun 15	Elsevier	UK, NL, USA	2011	3659-68	http://www.ncbi.nlm.nih.gov/pubmed/21306905	

53	Modulation of the activity of histone acetyltransferases by long chain alkylidenemalonates (LoCAMs)	C. Milite	Bioorg Med Chem	19(12) Jun 15	Elsevier	UK, NL, USA	2011	3690-701	http://www.ncbi.nlm.nih.gov/pubmed/21292492	
54	Epigenetic profiling of the antitumor natural product psammaplin A and its analogues	J. García	Bioorg Med Chem	19(12) Jun 15	Elsevier	UK, NL, USA	2011	3637-49	http://www.ncbi.nlm.nih.gov/pubmed/21215647	
55	Histone deacetylase inhibitors: recent insights from basic to clinical knowledge & patenting of anti-cancer actions	V. Carafa	Recent Pat Anticancer Drug Discov	6(1) Jan	Bentham Science	NL, USA, Pakistan	2011	131-45	http://www.ncbi.nlm.nih.gov/pubmed/21110829	
56	Death receptor pathway activation and increase of ROS production by the triple epigenetic inhibitor UVI5008	A. Nebbioso	Molecular Cancer Therapeutics	10(12):2394-404 Dec. Epub 2011 Oct 6	American Association for Cancer Research	USA	2011	219 – 228	http://www.ncbi.nlm.nih.gov/pubmed/20639404	
57	Molecular pathways: the complexity of the epigenome in cancer and recent clinical advances	M. Conte	Clin Cancer Res	Aug 17[Epub ahead of print]	AACR, US		2012		http://www.ncbi.nlm.nih.gov/pubmed/22904103	
58	Trials with 'Epigenetic' Drugs: An Update.	A. Nebbioso	Molecular Oncology	IN PRESS	Elsevier	UK, NL, USA	2012			
59	MePR: a novel human mesenchymal progenitor model with characteristics of	M. Miceli		SUBMITTED			2012			

	pluripotency.									
60	Sirtuins as targets of anticancer therapeutic strategies	V. Carafa	54th anual meeting of the italian cáncer society: Mission Impossible	1-4 Oct	Instituto ortopédico Rizzoli-Bologna	IT	2012			

Section B (confidential)

TEMPLATE B1: LIST OF APPLICATIONS FOR PATENTS, TRADEMARKS, REGISTERED DESIGNS, ETC.			
Type of IP Rights: Patents, Trademarks, Registered designs, Utility models, etc.	Application reference(s) (e.g. EP123456)	Subject or title of application	Applicant (s) (as on the application)
Trademark	Pending	True Micro ChIP kit	Diagenode
Patent	Pending	Technology and methods L-ChIP and L-ChIP seq	UNINA2, RU
Patent	EP11305531.3	Linear DNA amplification	Gronemeyer, H., Pattabhiraman, S. &. Trindade, L.

TEMPLATE B2: OVERVIEW TABLE WITH EXPLOITABLE FOREGROUND					
Exploitable Foreground (description)	**Exploitable product(s) or measure(s)**	**Sector(s) of application**	**Timetable, commercial use**	**Patents or other IPR exploitation (licences)**	**Owner & Other Beneficiary(s) involved**

Report on societal implications

.

A General Information *(completed automatically when **Grant Agreement number** is entered.*

Grant Agreement Number:	221952
Title of Project:	**Development of Laser-Based Technologies and Prototype Instruments for Genome-Wide Chromatin ImmunoPrecipitation Analyses**
Name and Title of Coordinator:	Prof. Lucia Altucci

B Ethics

1. Did you have ethicists or others with specific experience of ethical issues involved in the project?	**O**	**Yes**
	X	**No**
2. Please indicate whether your project involved any of the following issues (tick box) :		
INFORMED CONSENT		
• Did the project involve children?	NO	
• Did the project involve patients or persons not able to give consent?	NO	
• Did the project involve adult healthy volunteers?	NO	
• Did the project involve Human Genetic Material?	NO	
• Did the project involve Human biological samples?	NO	
• Did the project involve Human data collection?	NO	
RESEARCH ON HUMAN EMBRYO/FOETUS		
• Did the project involve Human Embryos?	NO	
• Did the project involve Human Foetal Tissue / Cells?	NO	
• Did the project involve Human Embryonic Stem Cells?	NO	
PRIVACY		
• Did the project involve processing of genetic information or personal data (eg. health, sexual lifestyle, ethnicity, political opinion, religious or philosophical conviction)	NO	
• Did the project involve tracking the location or observation of people?	NO	
RESEARCH ON ANIMALS		
• Did the project involve research on animals?	NO	
• Were those animals transgenic small laboratory animals?	NO	

• Were those animals transgenic farm animals?	NO
• Were those animals cloning farm animals?	NO
• Were those animals non-human primates?	NO
RESEARCH INVOLVING DEVELOPING COUNTRIES	
• Use of local resources (genetic, animal, plant etc)	**NO**
• Benefit to local community (capacity building ie access to healthcare, education etc)	**YES**
DUAL USE	
• Research having potential military / terrorist application	NO

C Workforce Statistics

3 Workforce statistics for the project: Please indicate in the table below the number of people who worked on the project (on a headcount basis).

Type of Position	Number of Women	Number of Men
Scientific Coordinator	**1**	**0**
Work package leader	**1**	**3**
Experienced researcher (i.e. PhD holders)	**22**	**38**
PhD Students	**16**	**10**
Other	**88**	**109**

4 How many additional researchers (in companies and universities) were recruited specifically for this project?	
Of which, indicate the number of men:	
Of which, indicate the number of women:	

D Gender Aspects

5	**Did you carry out specific Gender Equality Actions under the project** ?	**X** ○	Yes No

6 Which of the following actions did you carry out and how effective were they?

		Not at all effective				Very effective
❑	Design and implement an equal opportunity policy	○	○	○	○	**X**
❑	Set targets to achieve a gender balance in the workforce	○	○	○	**X**	○
❑	Organise conferences and workshops on gender	**X**	○	○	○	○
❑	Actions to improve work-life balance	○	○	○	○	**X**
○	Other:					

7 Was there a gender dimension associated with the research content – i.e. wherever people were the focus of the research as, for example, consumers, users, patients or in trials, was the issue of gender considered and addressed?

○ Yes- please specify

X No

E Synergies with Science Education

8 Did your project involve working with students and/or school pupils (e.g. open days, participation in science festivals and events, prizes/competitions or joint projects)?

○ Yes- please specify

X No

9 Did the project generate any science education material (e.g. kits, websites, explanatory booklets, DVDs)?

X Yes- please specify (kits, websites, explanatory booklets)

○ No

F Interdisciplinarity

10 Which disciplines (see list below) are involved in your project?

X Main discipline[3]: 1, 2, 3

○ Associated discipline[3]: ○ Associated discipline[3]:

[3] Insert number from list below (Frascati Manual)

G Engaging with Civil society and policy makers

11a	**Did your project engage with societal actors beyond the research community?** *(if 'No', go to Question 14)*	○ **X**	Yes No

11b If yes, did you engage with citizens (citizens' panels / juries) or organised civil society (NGOs, patients' groups etc.)?

- ○ No
- ○ Yes- in determining what research should be performed
- ○ Yes - in implementing the research
- ○ Yes, in communicating /disseminating / using the results of the project

11c	**In doing so, did your project involve actors whose role is mainly to organise the dialogue with citizens and organised civil society (e.g. professional mediator; communication company, science museums)?**	○ **X**	Yes No

12 Did you engage with government / public bodies or policy makers (including international organisations)

- **X** No
- ○ Yes- in framing the research agenda
- ○ Yes - in implementing the research agenda
- ○ Yes, in communicating /disseminating / using the results of the project

13a Will the project generate outputs (expertise or scientific advice) which could be used by policy makers?

- ○ Yes – as a **primary** objective (please indicate areas below- multiple answers possible)
- ○ Yes – as a **secondary** objective (please indicate areas below - multiple answer possible)
- **X** No

13b If Yes, in which fields?

Agriculture		Energy		Human rights	
Audiovisual and Media		Enlargement		Information Society	
Budget		Enterprise		Institutional affairs	
Competition		Environment		Internal Market	
Consumers		External Relations		Justice, freedom and security	
Culture		External Trade		Public Health	
Customs		Fisheries and Maritime Affairs		Regional Policy	
Development Economic and Monetary Affairs		Food Safety		Research and Innovation	
Education, Training, Youth		Foreign and Security Policy		Space	
Employment and Social Affairs		Fraud		Taxation	
		Humanitarian aid		Transport	

13c If Yes, at which level?

- ○ Local / regional levels
- ○ National level
- ○ European level
- ○ International level

H Use and dissemination

14 How many Articles were published/accepted for publication in peer-reviewed journals?		**60**
To how many of these is open access[4] provided?		
How many of these are published in open access journals?		
How many of these are published in open repositories?		
To how many of these is open access not provided?		
Please check all applicable reasons for not providing open access:		
❑ publisher's licensing agreement would not permit publishing in a repository ❑ no suitable repository available ❑ no suitable open access journal available ❑ no funds available to publish in an open access journal ❑ lack of time and resources ❑ lack of information on open access ❑ other: ……		
15 How many new patent applications ('priority filings') have been made? *("Technologically unique": multiple applications for the same invention in different jurisdictions should be counted as just one application of grant).*		**1**
16 Indicate how many of the following Intellectual Property Rights were applied for (give number in each box).	Trademark	
	Registered design	
	Other	
17 How many spin-off companies were created / are planned as a direct result of the project?		**NONE**
Indicate the approximate number of additional jobs in these companies:		

18 Please indicate whether your project has a potential impact on employment, in comparison with the situation before your project:

X	Increase in employment, or	❑	In small & medium-sized enterprises
❑	Safeguard employment, or	❑	In large companies
❑	Decrease in employment,	❑	None of the above / not relevant to the project
❑	Difficult to estimate / not possible to quantify	❑	

19 For your project partnership please estimate the employment effect resulting directly	*Indicate figure:*

[4] Open Access is defined as free of charge access for anyone via the internet.

from your participation in Full Time Equivalent (*FTE = one person working fulltime for a year*) jobs:	
Difficult to estimate / not possible to quantify	❑

I Media and Communication to the general public

20 As part of the project, were any of the beneficiaries professionals in communication or media relations?

X Yes ○ No

21 As part of the project, have any beneficiaries received professional media / communication training / advice to improve communication with the general public?

X Yes ○ No

22 Which of the following have been used to communicate information about your project to the general public, or have resulted from your project?

❑	Press Release	❑	Coverage in specialist press
❑	Media briefing	❑	Coverage in general (non-specialist) press
❑	TV coverage / report	❑	Coverage in national press
❑	Radio coverage / report	❑	Coverage in international press
X	Brochures /posters / flyers	X	Website for the general public / internet
X	DVD /Film /Multimedia	X	Event targeting general public (festival, conference, exhibition, science café)

23 In which languages are the information products for the general public produced?

❑	Language of the coordinator	X	English
❑	Other language(s)		

***Question F-10*:** Classification of Scientific Disciplines according to the Frascati Manual 2002 (Proposed Standard Practice for Surveys on Research and Experimental Development, OECD 2002):

FIELDS OF SCIENCE AND TECHNOLOGY

1. NATURAL SCIENCES

1.1 Mathematics and computer sciences [mathematics and other allied fields: computer sciences and other allied subjects (software development only; hardware development should be classified in the engineering fields)]

1.2 Physical sciences (astronomy and space sciences, physics and other allied subjects)

1.3 Chemical sciences (chemistry, other allied subjects)

1.4 Earth and related environmental sciences (geology, geophysics, mineralogy, physical geography and other geosciences, meteorology and other atmospheric sciences including climatic research, oceanography, vulcanology, palaeoecology, other allied sciences)

1.5 Biological sciences (biology, botany, bacteriology, microbiology, zoology, entomology, genetics, biochemistry, biophysics, other allied sciences, excluding clinical and veterinary sciences)

2 ENGINEERING AND TECHNOLOGY

2.1 Civil engineering (architecture engineering, building science and engineering, construction engineering, municipal and structural engineering and other allied subjects)

2.2 Electrical engineering, electronics [electrical engineering, electronics, communication engineering and systems, computer engineering (hardware only) and other allied subjects]

2.3. Other engineering sciences (such as chemical, aeronautical and space, mechanical, metallurgical and materials engineering, and their specialised subdivisions; forest products; applied sciences such as geodesy, industrial chemistry, etc.; the science and technology of food production; specialised technologies of interdisciplinary fields, e.g. systems analysis, metallurgy, mining, textile technology and other applied subjects)

3. MEDICAL SCIENCES

3.1 Basic medicine (anatomy, cytology, physiology, genetics, pharmacy, pharmacology, toxicology, immunology and immunohaematology, clinical chemistry, clinical microbiology, pathology)

3.2 Clinical medicine (anaesthesiology, paediatrics, obstetrics and gynaecology, internal medicine, surgery, dentistry, neurology, psychiatry, radiology, therapeutics, otorhinolaryngology, ophthalmology)

3.3 Health sciences (public health services, social medicine, hygiene, nursing, epidemiology)

4. AGRICULTURAL SCIENCES

4.1 Agriculture, forestry, fisheries and allied sciences (agronomy, animal husbandry, fisheries, forestry, horticulture, other allied subjects)

4.2 Veterinary medicine

5. SOCIAL SCIENCES

5.1 Psychology

5.2 Economics

5.3 Educational sciences (education and training and other allied subjects)

5.4 Other social sciences [anthropology (social and cultural) and ethnology, demography, geography (human, economic and social), town and country planning, management, law, linguistics, political sciences, sociology, organisation and methods, miscellaneous social sciences and interdisciplinary , methodological and historical S1T activities relating to subjects in this group. Physical anthropology, physical geography and psychophysiology should normally be classified with the natural sciences].

6. HUMANITIES

6.1 History (history, prehistory and history, together with auxiliary historical disciplines such as archaeology, numismatics, palaeography, genealogy, etc.)

6.2 Languages and literature (ancient and modern)

6.3 Other humanities [philosophy (including the history of science and technology) arts, history of art, art criticism, painting, sculpture, musicology, dramatic art excluding artistic "research" of any kind, religion, theology, other fields and subjects pertaining to the humanities, methodological, historical and other S1T activities relating to the subjects in this group